André Manuel Fernandes Coelho

Licenciado em Ciências da Engenharia Eletrotécnica e de Computadores

Solar rotation speed by detecting and tracking of Coronal Bright Points

Dissertação para obtenção do grau de mestre em

Engenharia Eletrotécnica e de Computadores

Orientador: Professor Doutor André Teixeira Bento Damas Mora, Professor Auxiliar, FCT-UNL

Co-orientador: Professora Doutora Maria Rita Sarmento de Almeida Ribeiro, Professora Associada Convidada, FCT-UNL

Júri

Presidente:

Arguente:

Membros:

Março 2017

FACULDADE DE CIÊNCIAS E TECNOLOGIA
UNIVERSIDADE NOVA DE LISBOA

Solar rotation speed by detecting and tracking of Coronal Bright Points

To my family, friends and Alexandra.

Acknowledgments

First and foremost, I have to thank my dissertation supervisors Dr. André Mora and Dr. Rita Ribeiro. Without their assistance and dedicated involvement in every step throughout the process, this dissertation would have never been accomplished.

It is unflattering not being able to describe how much effort, dedication and supervision Dr. André Damas Mora provided me and to this dissertation. It is truly an honor to be supervised by Dr. André and I believe I have learned so much from him which led me to admire him even further. I guess the best compliment I could give would be that there's no better person to have as your dissertation supervisor and I strongly believe that if there's a role model to follow, Dr. André is that person. Through countless hours of Q&A, problem solving headaches and even nonsenses from my behalf, Dr. André showcased the patience to put up with all of this and I would deeply like to thank him for everything he has done for me. Thank you!

To my co-advisor Dr. Rita Ribeiro. Thank you so much for this topic proposal, the willingness and the support throughout all stages. Being allowed to work in a subject that I am passionate about really helped boosting my commitment. Thank you for the unforgettable experience in Slovakia. The opportunity to develop my work alongside astrophysicists allowed me to grow as a person and as a student which I couldn't be more grateful. These examples are just a glimpse of a far more rewarding acknowledgement that I ought to give. Nevertheless, my deeply thanks to you.

I am very grateful to Dr. Ivan Dorotovic from the Slovak Central Observatory in Hurbanovo, Slovakia, and Dr. Jan Rybak from the Astronomical Institute of the Slovak Academy of Sciences in Tatranska Lomnica for supplying the SDO data, for valuable discussions and comments, as well as for the warm welcoming during my stay in Slovakia. It was an unforgettable

experience which I shall cherish for the rest of my life. I would also like to leave a word of appreciation for all the employees of the Slovak Central Observatory who received me so kindly and blessed me with the gift of friendship. Thank you!

This document finalizes my journey through university, but this journey was full of experiences and people that I have never truly thanked. Therefore, I want to show my gratitude to great mentors like Dr. José Manuel Fonseca, Dr. Helena Fino, Dr. José Barata, Dr. Mário Ventim, Dr. Paulo Pinto, Dr. Joaquim Pina, and Professor José Ferreira who taught me most importantly life lessons. Thank you *Faculdade de Ciências e Tecnologia da Universidade Nova de Lisboa* and everyone in it!

While family and friends are always there to back me up, cheer me up and encouraging me to fly higher when I feel I can´t even lift my own weight, I know there's someone else that supports me unconditionally, knows who I am and what I'm capable of, trusts me to overcome my challenges and is the first one to step in and raise me from wherever hole I dug myself into. She is and has been the light of my life, my first love and my model of integrity and responsibility and for all that, there is no thanks, there is a deeper feeling that only she knows. Alexandra Videira for your efforts, patience, love and caring throughout most of my university days I just hope I'm up to the task to make you feel the same way you make me feel. Love you!

Family is and will always be our safeguard. Firstly, I want to start by apologizing for not being able to finish this course sooner and for all the things I put you all through. In fact, it somehow made me realize how much I care, how much it hurts and how much I appreciate everything you do for me. Often we do not appreciate the things around us until we lose them, therefore, I am taking this time to think in each one of you, mom, dad, sister, grannies, aunt, uncle and cousins for everything you represent in my life. For everyone, thank you so much!

To all my friends, (and please disregard the order, you all mean same, right?) Gonçalo Alves, João Lourenço, João Ralo, Gonçalo Oliveira, Nuno Ramos, José Ferreira and all your girlfriends that I may or may not know, but at least everyone gets happy! For the sake of this acknowledgement I do have more friends but I decided to state the name of the few who directly or indirectly encouraged me to finish my thesis and helped me to get there. Thank you very much!

A special mention to Joaquim Pereira and João Soares who I'm truly grateful to have met and to have shared so much unforgettable experiences throughout university. I can only hope this

friendship endures for many, many years… I think both you, while being so different, taught me so much, not only school related subjects but also professionally and personally. Despite acknowledging your emphasis in my life, I just have one question to ask: When is the next snow trip going to be?

Finally, a special mention to Rui Lino, Luis Palma Carlos and Flávio Silva. While from different backgrounds each one of you represent a great deal to me. Luis have been my long time best friend, who I respect so much and who I have looked up for since I was a kid. His personality and strength are unbelievable! I am really fortunate to have you as friend! Rui, on the other hand, represents a friendship built on mutual respect and admiration that started and grew to be what it is today. Personally, I think we both appreciate deeply that our paths crossed together and that we were able to grow side by side and build what I can only hope to be a lifelong relationship. Finally, Flávio is a recent friendship that I feel I have known for a long time. I think we both understand each other pretty well and despite disagreeing in some subjects, I am very fond of him. I believe that from everyone he was the one who helped me the most in my thesis and for that I'm really grateful and anxious to return the favor. Whatever path we follow that may set us apart, I truly hope our friendship prevails. Thank you all!

Abstract

Coronal Bright Points are one of many Solar manifestations that provide scientists evidences of its activity and are usually recognized by being small light dots, like scattered jewels. For many years these Bright Points have been overlooked due to another element of solar activity, sunspots, which drawn scientists full attention mainly because they were easier to detect. Nevertheless, CBPs as a result of a clear distribution across all latitudes, provide better tracers to study Solar corona rotation.

A literature review on CBPs detection and tracking unveiled limitations both in detection accuracy and lacking an automated image processing feature. The purpose of this dissertation was to present an alternative method for detecting CBPs using advanced image processing techniques and provide an automatic recognition software.

The proposed methodology is divided into pre-processing methods, a segmentation section, post processing and a data evaluation approach to increase the CBP detection efficiency. As identified by the study of the available data, pre-processing transformations were needed to ensure each image met certain specifications for future detection. The detection process includes a gradient based segmentation algorithm, previously developed for retinal image analysis, which is now successfully applied to this CBP case study. The outcome is the CBP list obtained by the detection algorithm which is then filtered and evaluated to remove false positives.

To validate the proposed methodology, CBPs need to be tracked along time, to obtain the rotation of the Solar corona. Therefore, the images used in this study were taken from 19.3nm wavelength by the AIA 193 instrument on board of the Solar Dynamics Observatory (SDO) satellite over 3 days during august 2010. These images allowed the perception of how CBPs angular rotation velocity not only depends on heliographic latitude, but also on other factors such as time.

From the results obtained it was clear that the proposed methodology is an effective method to detect and track CBPs providing a consistent method for its detection.

Keywords: coronalbright points, solar image, image processing, segmentation algorithms, object tracking, GPL.

Resumo

Os *Coronal Bright Points* são uma das muitas manifestações do sol, que fornecem aos cientistas evidências da sua atividade e são habitualmente reconhecidos por serem pequenos pontos brilhantes espalhados por toda a extensão do disco solar. Durante muitos anos, os *Coronal Bright Points* foram negligenciados devido a outro elemento da atividade solar, as manchas solares, que recolheram a atenção dos cientistas principalmente por serem mais fáceis de detetar. No entanto, devido á sua distribuição ao longo de todas as latitudes, fornecem melhores referencias para estudar a rotação da coroa solar.

Uma revisão da literatura sobre a deteção e rastreamento de *CBPs* revelou limitações tanto na precisão de deteção quanto na falta de um sistema automático de processamento de imagem. O objetivo desta dissertação é apresentar um método alternativo para a deteção de *CBPs* usando técnicas avançadas de processamento de imagem e fornecer um *software* de reconhecimento automático que pode não ser sempre exato, mas sim consistente.

A metodologia proposta é dividida em: pré-processamento, algoritmo de segmentação, pós-processamento e uma abordagem de avaliação de dados para aumentar a eficiência do processo. Conforme identificado pelo estudo dos dados disponíveis, eram necessárias transformações em cada imagem para garantir que cada uma correspondia a um conjunto de especificações pré-definidas antes da aplicação do algoritmo de segmentação. A deteção usa um algoritmo de segmentação denominado *Gradient Path Labeling (GPL)*, que foi previamente desenvolvido para análise de imagens da retina, e que agora é aplicado a outro caso de estudo. O resultado é uma lista de *CBPs* que é em seguida filtrada e avaliada para remover falsos positivos.

Para validar esta metodologia, foi necessário fazer o rastreamento destas manifestações de forma a obter a rotação da coroa solar. Para tal, foram usadas imagens com um comprimento de

onda de 19.3nm obtidas pelo instrumento *AIA* 193 a bordo do satélite *Solar Dynamics Observatory (SDO)* durante 3 dias em agosto de 2010, o que permitiu a perceção de como a velocidade de rotação angular dos *CBPs* não só depende da latitude heliográfica, mas também de outros fatores, como o tempo.

A partir dos resultados obtidos ficou claro que a metodologia proposta é um método eficaz para detetar e acompanhar os *CBPs* proporcionando um método consistente de deteção dos mesmos.

Palavras-chave: *coronal bright points*, imagens do Sol, processamento de imagem, algoritmos de segmentação, rastreamento de objetos, *GPL*.

Table of Contents

Table of Figures

Table of Tables

Acronyms

AIA	- Atmospheric Imaging Assembly
BP	- Bright Point
CBP	- Coronal Bright Points
CME	- Coronal Mass Ejections
DIC	- Differential Interference Contrast
EIT	- Extreme Ultraviolet Imaging Telescope
EUV	- Extreme Ultraviolet
FITS	- Flexible Image Transport System
GPL	- Gradient Path Labeling
HAD	- Hazard Detection Avoidance
HMI	- Helioseismic and Magnetic Imager
IDL	- Interactive Data Language
JPEG	- Joint Photographic Experts
MDI	- Michelson Doppler Imager
PNG	- Portable Network Graphics
PSO	- Particle Swarm Optimization
RGB	- Red, Green and Blue
RIM	- Regional Intensity Maximum
SDO	- Solar Dynamics Observatory
SOHO	- Solar and Heliospheric Observatory
SOLA	- Subtractive Optimally Localized Averages
SWAMIS	- The Southwest Automatic Magnetic Identification Suite
TRN	- Terrain Relative Navigation

1 Introduction

In this chapter the author unveils the motivations behind this dissertation providing an important insight about the object of study, the Sun. It is relevant to define some key notions about the Sun in order to easily understand further discussed topics. Later on, the author outlines some obstacles that needed to be taken into account on image processing related subjects and on available equipment limitations concerning images captured.

It is noteworthy to mention that the scientific community does not, necessarily, have a scientific name for "our" Sun or "our" Solar System, thus being called by their common and respective names. However, as Jagadheep states (D.Pandian, 2016), stars are categorized by temperature and size which helps understanding Sun's profile related to other stars. Based on their temperature, they are classified by a set of letters (e.g. O, B, A, F, G, K and M) which "O" corresponds to the hottest temperature, whether the letter M represents the coolest temperature stars. These group of star classifications are also subdivided into 10 classes (e.g. O0, O1…). Regarding size, stars are classified into classes such as Ia, Ib, II, III, IV and V. Therefore, based on this notation, "our" star can be classified as a G2V star (D.Pandian, 2016).

Despite all the available literature about the Sun, such as scientific papers, specialized books in astrophysics and active observatory websites, the author highlights SolarHam website

(*http://www.solarham.net/*) which is routinely updated with accurate solar information. The web-site provides real time solar news, as well as data from different sources which is a valuable tool to support researchers.

This dissertation will focus on Coronal Bright Points (CBP) detection and tracking in Solar disk images. Like a few other solar surface manifestations, CBPs have the potential to be remarkable tracers and therefore, provide a good support to researchers in Solar studies. The following chapters will provide in depth knowledge about these structures and the methods to be applied.

1.1 Scope and Motivation

The motivation behind this dissertation lies on the importance of knowing Solar differential rotation which, according to present conceptions, plays a decisive role maintaining Solar magnetic fields and the whole Sun's activity (Brajša et al., 2001). The key point is that differential rotation mechanisms, most likely caused by interactions between the convection and the overall rotation are still being subject of studies and not fully understood. In fact, Solar differential rotation calculations need to be performed concerning the different layers of the Sun (explained in the next sub-chapter), where both solar surface and interior rotation still are an open issue for solar physicists (Shahamatnia, Dorotovič, Fonseca, & Ribeiro, 2016a). Therefore, the author aims to apply image processing algorithms to a sequence of images of the Solar disk, to improve the understanding of its differential rotation as a result of identifying and tracing Coronal Bright Points.

Coronal Bright Points or CBPs are sources of X-ray and ultraviolet emission which are recognized by being small dots of light, like scattered jewels. In fact, CBP's are associated with intense, localized magnetic fields of opposite polarities and, according to (Eddy, 1979), CBPs are a basic element of solar activity, perhaps as fundamental as the sunspots. Notwithstanding the similarities, it is in their disparity that makes CBPs increasingly more interesting. Sunspots are known to be found concentrated in two mid-latitude bands on either side of the equator (Redd, 2015), whereas CBPs can be found all over the Sun, even appearing at the poles and in coronal holes. This unique feature allow researchers, after detecting and tracking CBPs over a sequence of images, to understand Solar rotational speed, which is known to be different for different latitudes and longitudes (Davor Sudar, Saar, Skokić, Beljan, & Brajša, 2016). Another important feature is that CBPs are numerous in all phases of the solar cycle which facilitate measurements of solar rotation based on the selected tracers. In contrast, sunspots depend on the solar cycle, therefore, it is almost impossible to obtain Sun's differential rotation profile during solar minimum (D. Sudar, Skokic, Brajša, & Saar, 2015).

Since one of the main objectives is to calculate Solar rotational profile it is important to understand why is that important.

There are several reasons to study the Sun (Thompson, 2004). Firstly, it is the only star that can be observed in detail, providing an important input about stellar structure and evolution. Secondly, the Sun's influence on Earth, without it, life wouldn't exist and with it the constant flow of particles and radiation being expelled in every direction affect our planet dynamic and environment, thus the importance of understanding solar-terrestrial relations. Thirdly, Sun provides a unique laboratory for studying fundamental physical processes in conditions that cannot be replicated on Earth. Some of those studies were about manifestations of convective motions and acoustic and gravity waves, which can be found in (Deubner, 1975).

Regarding internal rotation, the term itself, "rotation", is ubiquitous in astrophysical systems as (Thompson, Christensen-Dalsgaard, Miesch, & Toomre, 2003) states. During a system's formation as a result of gravitational contraction, its moment of inertia is reduced and therefore, any initial rotation is greatly enhanced. Often the evolution of this rotation is linked with the evolution of the magnetic field, therefore, understanding these processes is essential for a description of this type of phenomena's. Due to the fact that these processes are poorly understood by astrophysics, it increases the difficulty in developing efficient image processing systems that provide the necessary detailed insights. Further, there are consistent surface rotation deductions from spectroscopic observations and from measurements of magnetic features motions such as sunspots or CBP's - the tracking Solar feature addressed in this dissertation.

Figure 1, illustrates Solar rotation based on SOLA (Subtractive Optimally Localized Averages) inversion technique.

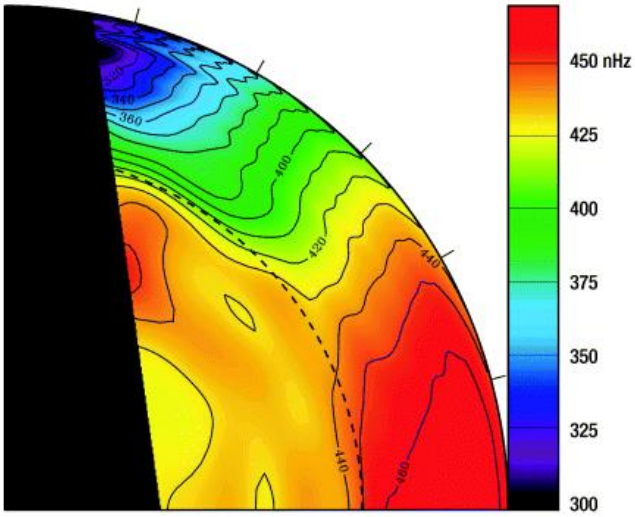

Figure 1: The rotation rate inside the Sun inferred from MDI data. The equator is at horizontal axis and the pole is at the vertical axis. The black shaped form in the figure represents lack of data and should be discarded from analysis. Image courtesy of (Thompson et al., 2003).

Figure 1 provides an important insight about the internal rotation based on oscillations, which are predominantly standing acoustic waves or surface-gravity waves. In the convection zone the rotation varies principally with latitude and rather little with depth, although with significant subtler details. Amongst these is the near-surface shear layer, where the rotation increases with depth. The radiative interior, on the other hand, rotates at a uniform rate. The transition between these two regimes takes place in a narrow region, called tachocline, where according to (Thompson et al., 2003) is widely believed to be the large-scale magnetic field generation by dynamo action and where is evident a strong radial rotational shear.

The Sun's profile shown in Figure 1, suggests that the rotation in the convection zone be "constant in cylinders", as Thomson states, thus, "*there must be processes that redistribute angular momentum in the convection zone, resulting in the observed profile*". With this in mind, it is obvious that different methods provide hints on Solar rotation and the motivation for this dissertation is propelled by the achievement of contributing to this issue.

More in line with the technologies to be used in this dissertation, the images provided by, for example, Solar Dynamics Observatory (SDO) that carries modules like Atmospheric Imaging Assembly (AIA) and Helioseismic and Magnetic Imager (HMI) ensure their applicability when developing robust and very efficient software to keep up with SDO data streams.

Figure 2 illustrates several CBP's detected by applying a BP finder algorithm to a full disk image of the Sun.

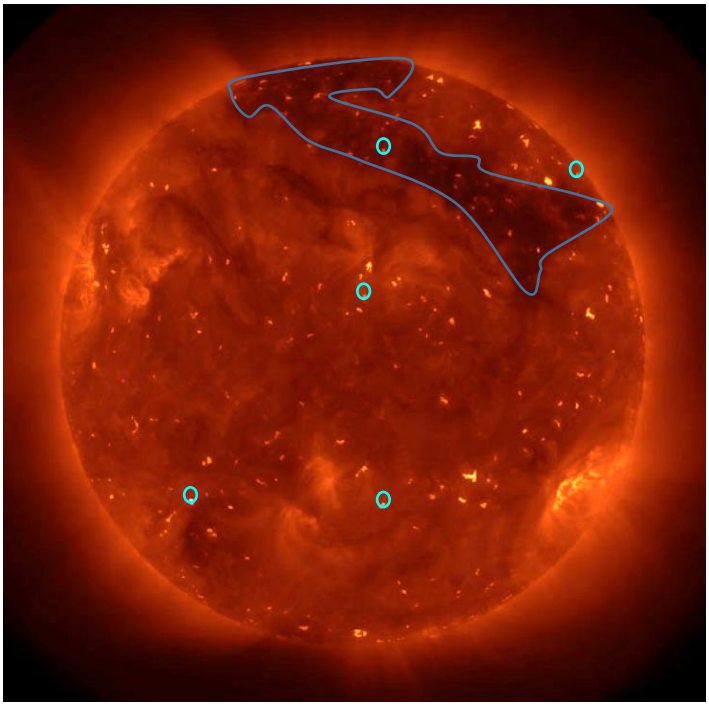

Figure 2: CBP's finder algorithm on a Full-disk image of the Sun. Coronal Bright Points have been highlighted from the background and appear similar to round shaped points in the Sun's disk. This figure was borrowed from (Martens et al., 2012) and was taken on 29 July 2010 at 15:27:56 UT.

It is perceivable in Figure 2 the amount of bright points that could be selected as potential markers, however, not all of them are suitable due to their specific lifetimes. In order to corroborate previous statements on this chapter, the image illustrates some CBP's locations (highlighted in light blue), across all latitudes and even in coronal holes - highlighted area in dark blue.

The author emphasizes the importance of automated feature recognition not only on astrophysics domain but also in a wide range of daily application scenarios, such as diagnosis of medical X-ray images, traffic jam' monitoring, security surveillance, between others (Acharya, 2005). In fact, not only the understanding of Sun's activity and its rotational profile motivated this dissertation but also the development of image processing algorithms that empower scientists with new tools to answer yet unsolved questions.

Regarding image processing point of view, the motivation is simple, it lies on applying new algorithms that produce better and more reliable results. The precision when detecting CBP's still has room to be improved, however, there are also several difficulties to address due to the particular nature of the CBP's, which have no specific shape and only last for a limited time, becoming harder to detect and evaluate if the sequence of images taken doesn't have a proper time interval between shots.

To help elucidating the struggle about finding and detecting CPB's, Figure 3 illustrates the complexity of Solar activity.

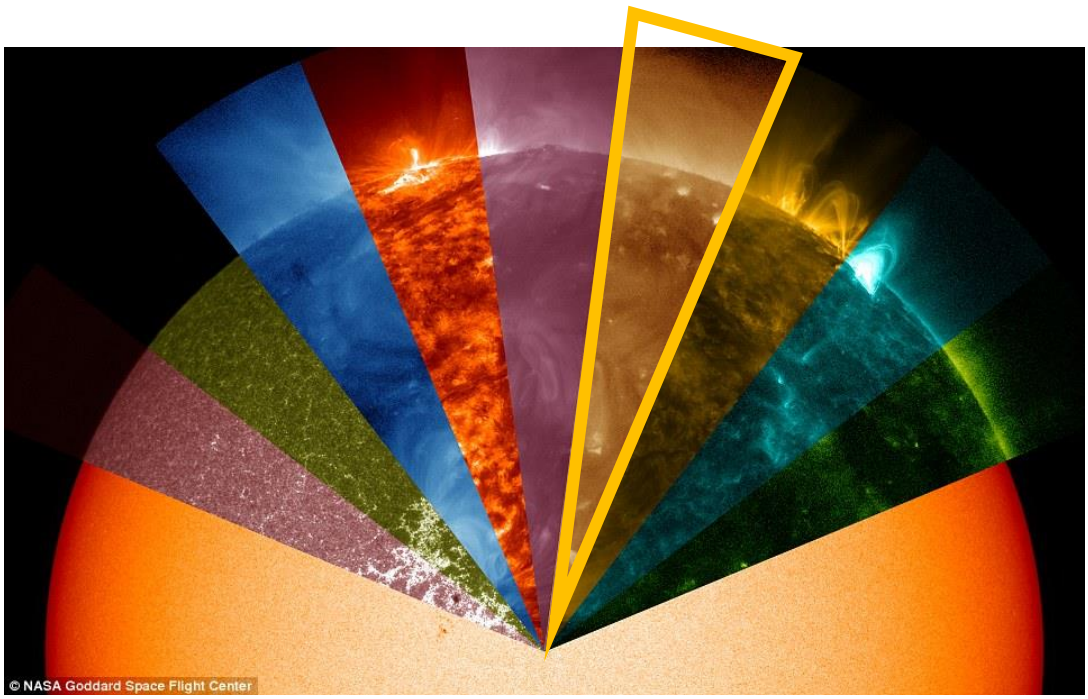

Figure 3: Sun's image with different wavelengths. NASA's SDO can see a wide range of wavelengths – invisible to the naked eye but converted and colorized into an image human eye can see (Prigg, 2015).

Regarding Figure 3, the golden colored triangle of the Sun is the one which more clearly helps detecting CBP's, which, again, can be identified by the round shaped bright points. Yet, CBP's are not easily detected due to their specific nature and occur along with other manifestations or phenomena's of the Sun. What is also noteworthy, is that NASA's SDO ability to produce images in a wide range of wavelengths which provides very high accuracy catalogs of solar features, most desirable assets for solar physicists (Martens et al., 2012). In fact, many studies have been limited by the fragmented nature of solar observations – different observatories, limited image cadence, and different time coverage – the result is that it is harder to find models capable of being applied to different cases, converging every single model to a specific solar manifestation.

It is very important to detect, trace, analyze and understand numerous phenomena's that the Sun is constantly producing. Despite being a primary source of energy for Humanity, it can also be a menace due to its unpredictable activity. Subject to the different wavelength images, many of following phenomena's can be seen in Figure 3, including flares, sigmoid, filaments, coronal dimming, polarity inversion lines, sunspots, Coronal Bright Points, active regions, coronal holes, coronal mass ejections (CMEs), coronal oscillations, between others (Martens et al.,

2012). For the purpose of this dissertation, as previously stated, the focus will be on CBP's identification which is believed to offer the best results as a valuable source of information regarding Sun's differential rotation.

1.2 The Sun

Our Sun is the object of studies due to its immense value as a primary source of energy, therefore, it is important to continuously put effort on studying its properties and activities. In this topic the author's intention is to provide some definitions needed to properly understand various concepts across this dissertation.

To begin with, Figure 4 illustrates Sun's structure and a few of its activities. The objective of this image is to allow a broader view of the object of study.

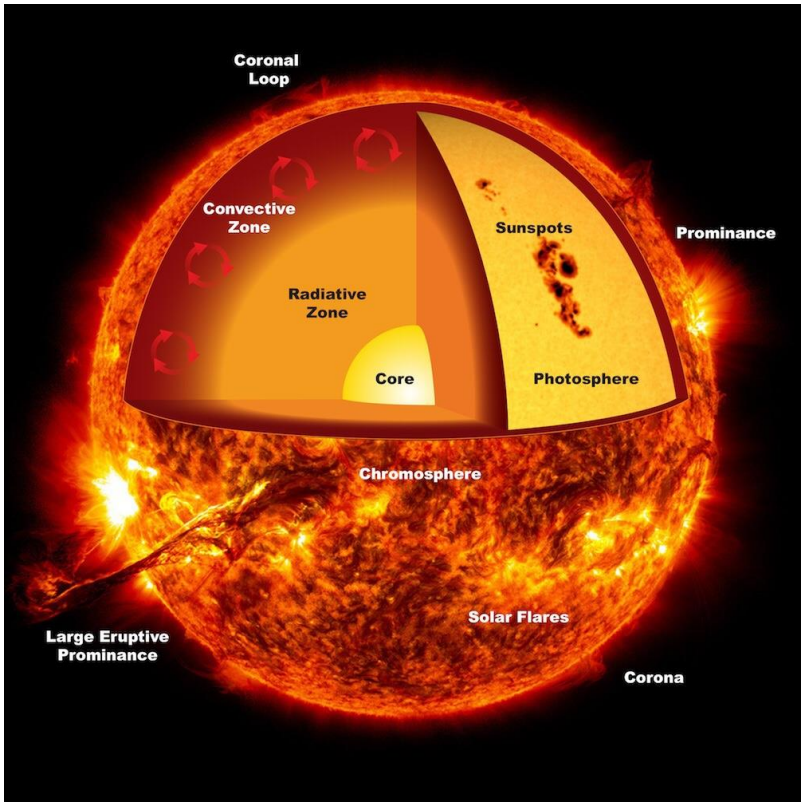

Figure 4: Sun's structure and activity. Figure borrowed from (ThinkLink, n.d.)

The Sun, as shown by the illustration above, can be divided into 6 layers. Starting from the center, the Core, the Radiative Zone, and the Convective Zone, then the upper layers are the Photosphere, the Chromosphere and finally the outmost layer, the Corona (SOHO, n.d.).

Regarding Sun's structure and activities should be defined the following concepts:

Photosphere

This layer is known for sunspots observations and it's the deepest layer observed directly. Its temperature varies between 6500K at the bottom and 4000K at the top and it is most covered by a form of granulation (Zell, 2015).

Chromosphere

This layer has an interesting property that unlike other layers the temperature raises as further way from the Sun's center. The temperature varies between 4000K to 8000K at the top (Zell, 2015). It is known for solar flares observations.

Corona

Corona is the outmost layer of the Sun and has a temperature of about 500.000K up to a few million K. With no upper limit, this layer cannot be seen with the naked eye except during a total solar eclipse or with a coronagraph (Zell, 2015). This layer is known for Coronal Bright Points observations.

Active Regions

Active Regions in solar atmosphere have intense magnetic fields that emerge from the surface layers to form loops which extend to the corona. Often destabilizations occur due to external forces such as flux emergences and the system stored energy could be suddenly released as accelerated particles and an increase in solar eruptions, for example flares and coronal ejections (Moon et al., 2016).

Coronal Bright Points

CBP's as they are currently known, are small and bright structures observed in extreme ultraviolet (EUV) and in X-ray frequencies of the solar spectrum. These bright points have a typical area of 2×10^8 km^2 and mean lifetime around 8 hours (Shahamatnia, Dorotovič, Fonseca, & Ribeiro, 2016b), however, literature review about CBP's lifetime does not uniformly agree on a precise lifetime, therefore, due to the lack of consensus, the author highlights the several lifetime discrepancies and the importance of deciding which CBP's provide the best tracers. One of its important features is how often these occurrences emerge over the Sun surface each day and across all latitudes. CBP's are found to be associated with magnetic fields of opposite polarities located in the photosphere. According to (Chandrashekhar, Prasad, Banerjee, Ravindra, & Seaton, 2012), one third of CBP's lie over ephemeral regions, which are newly emerging regions of magnetic flux, whether the other two thirds lie above canceling magnetic features, which consist of opposite

polarity fragments that approach one another and disappear. Another interesting point (Chandrashekhar et al., 2012) refers is the shorter lifetimes for some bipoles seen by X-ray than EUV. Further into Chandrashekhar et al, document, it is found an explanation for this which summarily states that temperature depends strongly on the magnetic energy released and, therefore, on the bipole magnetic-field strength. It also elucidate that not only coronal emissions rise due to an increase in emission area but also because CBP's emit more per unit area as the magnetic flux becomes stronger. Yet these effects only occur when CBP's are on growing or decaying phase, which means for the brightest moment of its lifetime, where there is an increased emission does not accompany by a comparable increase in the magnetic flux. Finally, there are studies that refer that there are different types of CBP's, ones associated with the ephemeral regions and others called classical CBP's, which do not exhibit significant evolution in their magnetic and coronal structure.

Sunspots

Sunspots, according to (Shahamatnia, Dorotovič, Mora, Fonseca, & Ribeiro, 2015), are the easiest features to detect from all manifestations of solar activity. Commonly seen as dark areas in Sun's photosphere, cooler than their surroundings, grown in importance due to their nature, which are associated with strong magnetic fields and through tracking systems provide solar physicists valuable insight and raw data about solar cycle. One of the advantages of using sunspots is a very long time coverage. On the other hand, there are numerous disadvantages: often complex structures, non-uniform distribution, which do not extend to higher latitudes, and the number of sunspots is highly variable during the solar cycle (D. Sudar et al., 2015).

Another relevant aspect about sunspots is the how they are classified. The Zurich classification scheme uses nine main classes according to the size of sunspots and their distribution inside a group. The Mount Wilson classification scheme sorts and groups sunspots according to their magnetic structure into four main classes, that is, on relative locations, size of concentrations and opposite polarity magnetic flux (Moon et al., 2016). For more detailed classification other schemes are being used such as McIntosh classification containing 60 classes.

Solar Cycle

The Solar Cycle is measured by the amount of magnetic flux that rises up to the Sun surface, the amplitude and configuration of which vary with time. Studies conducted revealed that the formation and decay of strong magnetic fields results in variations in electromagnetic radiation, sunspots and intensity of plasma flow (Popova, 2015). The Solar Cycle is also referred as the sunspot cycle because is directly correlated with the number of sunspots across the photosphere. For instance, in its minimum the sunspots are rarely seen despite small and side short life occurrences

and in its maximum there will be several appearances with large diameter and last many weeks. Regarding the studies about the number of sunspots on Sun's surface, Dr. Helen Popova clarifies there exists a cyclic structure that vary in every 11 years, which is commonly used to represent the average duration of the Solar Cycle.

Coronal Mass Ejections

CMEs are huge explosions of magnetic field and plasma from the Sun's corona. This ejections are undisputedly important to track and study due to their responsibility for geomagnetic storms and enhanced auroras when impacting with Earth's magnetosphere. CME's originate from twisted magnetic field structures, often visualized by their associated filaments or prominences. When this twisted structures erupt from active regions, they are often accompanied by large solar flares, which travel in every direction from the Sun to its surroundings. At present time, the magnetic field cannot be determined until it is measured as the CME passes through a monitoring satellite, leaving this occurrences to hit Earth's tiny magnetosphere, which protect our planet's life from perishing.

Focusing on the purpose of this dissertation which is the calculation of the Solar rotation profile, according to literature, the Sun rotates around its axis once in about 27 days. This rotation was first detected by observing the motion of sunspots but since the Sun is a giant, rotating cloud of gas it does not rotate rigidly like other solid planets. In fact, Sun's equatorial rotation is faster, approximately 24 days, then Polar Regions, which rotate once in more than 30 days (NASA, n.d.). In order to precisely measure its rotation several studies are currently under research and new methods of providing data to astrophysics being developed.

1.3 Research Problem

Considering a given image of the Sun's disk is perfectly taken, i.e. with an optimal resolution and well defined CBP's, the identification and detection of them would be rather simplified. Therefore, applying an automated algorithm that provides precise CBP's locations over a sequence of optimal resolution images will improve efficient calculations of Sun's differential rotation, with a minimum margin of error.

However, due to CPB's nature, previously discussed (e.g. their lifetime differs from each other), sometimes the results provide inaccurate detection and tracking. Regarding this issue, a solution might be to perform a selection from all the CBP tracers to choose the best results. Other factors to be taken in consideration are the necessity to improve the algorithm performance and

the hardware available because those type of images often require powerful processors and graphic cards to produce results as faster as possible.

Ideally, the research approach for detecting and tracking CBP's would be accomplished by applying 5 steps:

- **Detection** in which features are identified for each image.
- **Identification** in which the detected features are given unique IDs.
- **Association** in which the detected features in an image are given a secondary ID in order to link the feature with the succeeding images feature. This allows tracking throughout its lifetime.
- **Selection** in which its given additional information about coordinates, center of mass and other relevant details.
- **Conclusion** in which are given the summarized version of the process, optimized and prepared for future uses.

The above approach is based on the model presented by SWAMIS (The Southwest Automatic Magnetic Identification Suite) (DeForest & Lamb, 2014).

Each step has its own challenges to overcome, however, the first one is critical for the overall success of the process. Automatic recognition software provides an important tool to reduce subjectivity, as previously mentioned, coronal bright points appear along with other solar activities, therefore, even amongst experts should be seen some disagreement about its identification. With this in mind, it does not mean that automatic recognition software is always accurate but at least it should be consistent. The developer should identify a set of features that provide the best possible identification and then, based on those, collect every existent CBP and repeat the process for the upcoming sequence of images.

The first research question addressed in this dissertation is then: why are CBP's difficult to detect or why is there subjectivity related to their identification?

The answer to these questions lies not only on our knowledge about the phenomena but also on the available images provided by satellites. Fortunately, satellites supply images from different wavelengths are now allowing researchers to play with different combinations and retrieve the most information out of them. One of the major factors about consistently retrieving good results when identifying CBP's is working towards a reproducible method, which demands establishing a common mechanism or process to detect CBP's. There are several ways in order to accomplish this, for instance, detecting a specific type of contour/shape, even so this might possibly increase the difficulty, due to other events overlapping the CBP or the own CBP exhibit

irregular shapes, should be taken into account. Another approach could be about evaluating the location of the center of mass, which would most likely provide better precision, even if a threshold needed to be added afterwards. Given a certain Sun disk image it is noticeable the brightness disparities between different features, therefore, other possible approach would be to detect those variations in brightness and applying intensity thresholds, isolating the ones referring to CBP's. It is not always clear which method hand over the finest result and that's why it is so important to update the available mechanisms and algorithms to ensure progression.

The feature identification process will also undertake image segmentation to fulfill the purpose of identifying and tracking CBP's. Regarding segmentation, it can be defined as the process of partitioning the image into segments, labeling each pixel in order to understand which ones share the same characteristics (Yogamangalam & Karthikeyan, n.d.). The ultimate goal is to detect or locate objects and boundaries, which contribute for a clear analysis and in this particular case, of Coronal Bright Points.

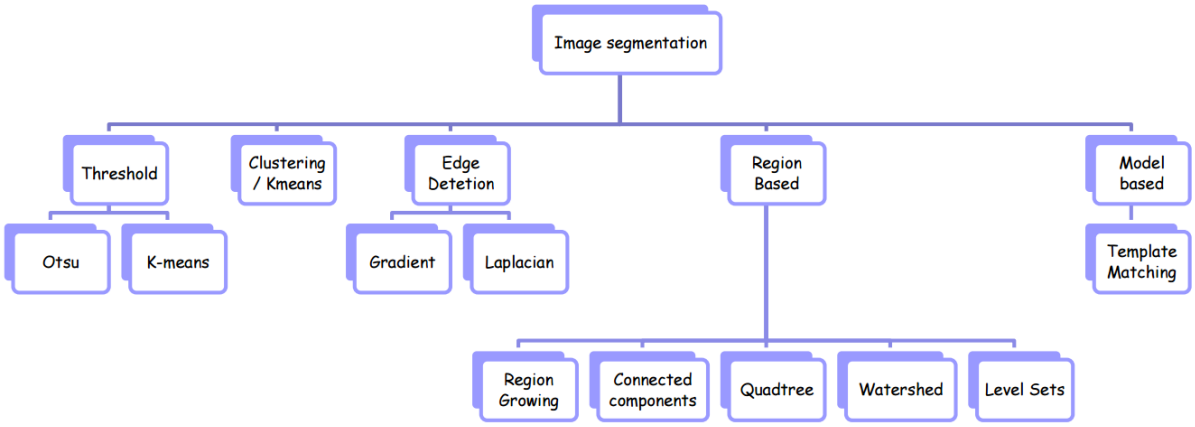

Figure 5: Image segmentation methods. Courtesy of Faculty professors André Mora and José Fonseca.

There are several methods for image segmentation, as illustrated in Figure 5, that reduce image information for easier analysis. Naturally, there are advantages and drawbacks for each of them, hence the necessity of performing a background study to identify their potential value in this case study. Superficially, based on previous experiences, the author identifies region based methods likely to be the most promising ones, especially Gradient Path Labeling (GPL) (A. D. Mora et al., 2011), which is a labeling algorithm like connected components, but with similar results as watershed algorithm (A. D. Mora et al., 2015). More about GPL and other segmentation methods will be clarified in the next chapter.

A second research question addressed in this dissertation is then: Is Gradient Path Labeling segmentation algorithm suitable to accurately detect CBP's?

1.4 Dissertation Outline

This dissertation features 5 chapters that provide an in depth knowledge about the work accomplished. Firstly, in this chapter was presented the scope and motivation, followed by Sun's structure and definition and the research problem. Afterwards, it is presented a set of chapters which are objectively prepared for supporting analysis and introspection. The five chapters' summaries are:

Introduction: Hosts the first impressions of the work developed. In this chapter the author targets the key points that led to pursue this challenge, both motivational aspects and daily basis endeavors of scientists which would benefit from this work. Moreover, it is presented the research problem and ways to tackle the challenge. Finally, the dissertation timeline is depicted

State-of-the-Art: This chapter aims to review some algorithms for detecting and tracking Coronal Bright Points. Should be looked upon as a background research study on existent algorithms with emphasis on detection and tracking, highlighting their potential, improvements and drawbacks. At the end of the chapter, the author presents a general conclusions section which targets the key subjects addressed in this chapter.

Implementation: At this stage, it is revealed the methods and techniques used in this dissertation. Firstly, a quick review on image formats and some explanations about the dataset used. Secondly, the methodology shaped to successfully tackle all the previously set obstacles is suggested and includes pre-processing methods, a segmentation section and a post processing methods to increase the CBP detection efficiency. Finally, a thorough explanation of each step of the methodology is presented.

Results Assessment: This chapter summarizes the results obtained, equations and methods to retrieve the solar rotation profile.

Conclusions and Future Work: Conclusion of the dissertation states the outcome of the experiments conducted and evaluates the results obtained. It proposes also topics which would most likely improve this subject to achieve better results or complement with additional features the developed software.

2 State-of-the-Art

Studies of solar rotation profile are either based on tracing specific solar features or by applying Doppler measurements and equations (Davor Sudar et al., 2016). This chapter appeals to the acknowledgement of different algorithms and thought processes behind identifying and tracking solar features. Aforementioned in the previous chapter, there are several features in the Sun, however, only some provide hints on Solar rotation profile. Traditionally, sunspots were the principal object of research to understand Solar rotation and by understanding sunspots lifetime today's solar cycle is defined by them. In fact, sunspots are the oldest tracers known for that purpose and studies are dated since 1951 according to (Davor Sudar et al., 2016). Nonetheless, this dissertation and many others related with the same subject, shifted their sight to another feature which is believed to produce better results – Coronal Bright Points (CBP's) – as previously mentioned, their arrangement across the solar disk should be of a greater value as a tracer to understand The Sun rotation profile.

This review is mostly directed to image processing methods which provide astrophysicists and other scientist's tools to improve their knowledge about a determined subject. The challenge lies on developing methods using digital image processing that can consistently detect and trace CBP's on solar disk images. These methods are not only used to detect their presence but also to

confirm their value as a tracer, therefore, providing additional intelligence about their size, life-time, number and type. Yet again, the major goal of these methods is the repeatability factor, maintaining a pre-defined criteria to reducing subjectivity.

2.1 Detection Methods

The selected algorithms presented in the following sub-chapters should provide a clear insight about advantages and drawbacks about their specific applications. Additionally, it is expected to enlighten about the thought process, aiming to corroborate best practices when detecting features using digital image processing methods.

2.1.1 GPL

Gradient Path Labelling is a promising segmentation algorithm that combines both connected components and watershed transform. GPL is commonly used for detecting zones with maximum or minimum intensity and it accomplishes that by using an image gradient as the basis of a pixels' labelling procedure, like (A. Mora, 2010) states. However, despite GPL algorithm been developed to fulfil a different role due to the nature of the case study presented by (A. Mora, 2010), the author of this dissertation believes GPL could be used to identify CBP's in an image of the Sun's disk.

The principle of the Gradient Path Labeling suggests that, alike a mountain climb, one or more paths reach the same maximum intensity. Therefore, the confluence of several significant ascending paths means that it should be present a regional intensity maximum (RIM). Regarding

, it illustrates the previous principle by looking into an image gradient in a velocity plot (also called quiver plot).

What is aimed to be obtained from this is a segmented image, where the features, intended to be detected, stay isolated from each other. Firstly, the algorithm detects RIM and areas of influence, collections of pixels which belong to the feature's ascending path, Later on, it groups ascending paths from the same RIM and produces a segmented image, seen in b). The output is an image with better segmentation and less complexity making it, overall, an optimized process.

In order to further understand GPL it is important to acknowledge the two stages of this method, Labelling and Labels Merging.

As (A. Mora, 2010) explains, the first stage is Labelling, a procedure that assigns to pixels with similar features a common label. Usually, to evaluate ascending paths, GPL procedure uses the gradient image, which main advantage is the analysis of pixel's 3×3 neighborhoods that remove several noise related artefacts. To achieve this operation, the most common methods are edge detection methods, such as Roberts or Sobel filters. Yet again, the output can be seen in Figure 6, being highlighted the maximum and minimum intensity pixels.

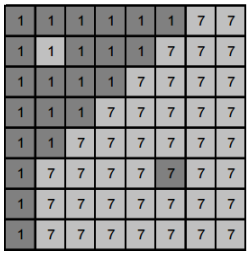

Figure 6: Final Labelling output image

It is also noteworthy, according to (A. Mora, 2010), that the complexity and time consumption of the algorithms implementation is approximately linear to the image's size, which is considered an advantage.

Further into the algorithms analysis, often after the first stage, the generated image appears to be over-segmented. Consequently, to overcome this drawback, a second stage is introduced – Labels Merging – which due to the existence of plateaus (flat hills) not all gradient paths end on the same RIM. Despite achieving good results with the solution for plateaus problem from Watershed Transform, a merging algorithm was adopted. (A. Mora, 2010) merging algorithm "*is based on the analysis of the paths with higher intensity between the RIM and each of its neighbors. The merging condition is for the path's amplitude difference to not exceed a predefined value*". What this allows is an algorithm which can output different images based on a parameter that defines the level of detail of the analysis.

For comparison purposes, Figure 7 provides a clear illustration of the differences between Watershed Transform and GPL, seen in b) and d) and, both stages of GPL method seen in c) and d). Both algorithms have similar tendencies on less complex, smoother images, nevertheless, Watershed Transform has a higher tendency for over-segmentation. Another key point stated by (A. Mora, 2010) is that GPL output provides a robust object detection with relatively good execution times. In fact, it is true that the merging algorithm adopted doubled the execution time but compensates in the algorithms final result which, fortunately, it still is faster than its contenders.

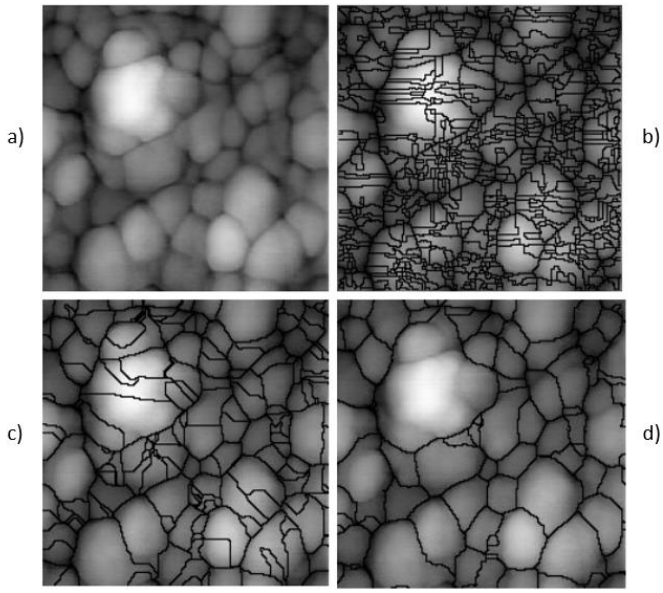

Figure 7: Comparison between Watershed T. and GPL. a) Original image, b) Watershed Transform, c) GPL segmentation without merge, d) GPL segmentation with merge. Courtesy of (A. Mora, 2010)

2.1.1.1 GPL Process

Finally, it should be discussed the thought processed behind GPL algorithm and its purpose. The following diagram, seen in Figure 8, illustrates the process step by step and should be acknowledge as a wide overview.

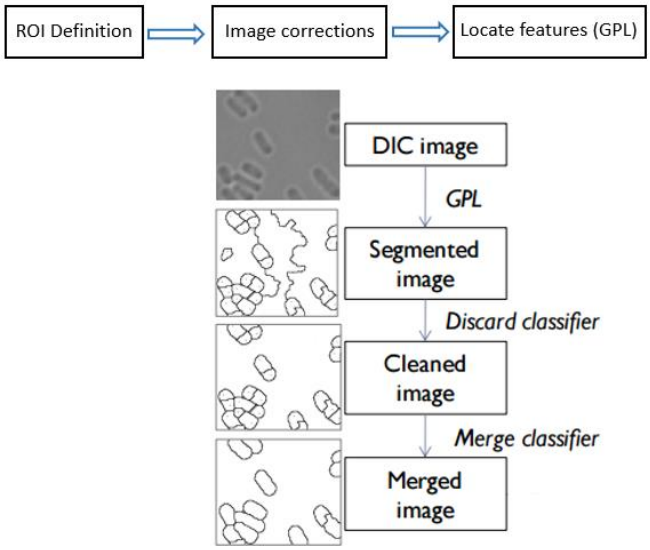

Figure 8: GPL process DIC stands for Differential Interference Contrast image. Image taken from FCT-UNL Advanced Topics on Image Processing course, 2016.

The case study presented in the images from Figure 8, is about GPL application in the detection and tracking of bacteria's and it summarizes and displays the final output of the algorithms implementation. The diagram itself is self-explanatory, however, it is essential to emphasize the early, pre-processing, procedures which help "cleaning" the image and also, in the later stages, the merging algorithm to reach the desired output.

As a final point (A. Mora, 2010) also states that GPL algorithm can be applied to other image processing scenarios, including sunspots which was already tested. Therefore, GPL should be considered an important tool for Coronal Bright Points detection.

2.1.2 BP-Finder Algorithm

BP-Finder Algorithm was first developed by (Gurman & McIntosh, 2004) and it is a variant of a former algorithm written in the interactive Data language (IDL) which exploits some of its features and include new ones. The algorithms recipe consists on taking a raw EIT FITS file, which stands for the Extreme ultraviolet Imaging Telescope on board of the SOHO (Solar and Heliospheric Observatory), and perform certain reduction steps such as dark current subtraction, degriding, filter normalization, exposure normalization, response correction, removal of stray light and others, all described in EIT User Guide. Further into this subject, (Gurman & McIntosh, 2004) explain objectively which other steps need to be performed in order to successfully detect CBP's. Some of these steps are related with removal of remaining bright lights, filtering background intensity, noise level calculations, deviations and rejection methods based on size and shape of the featured CBP's.

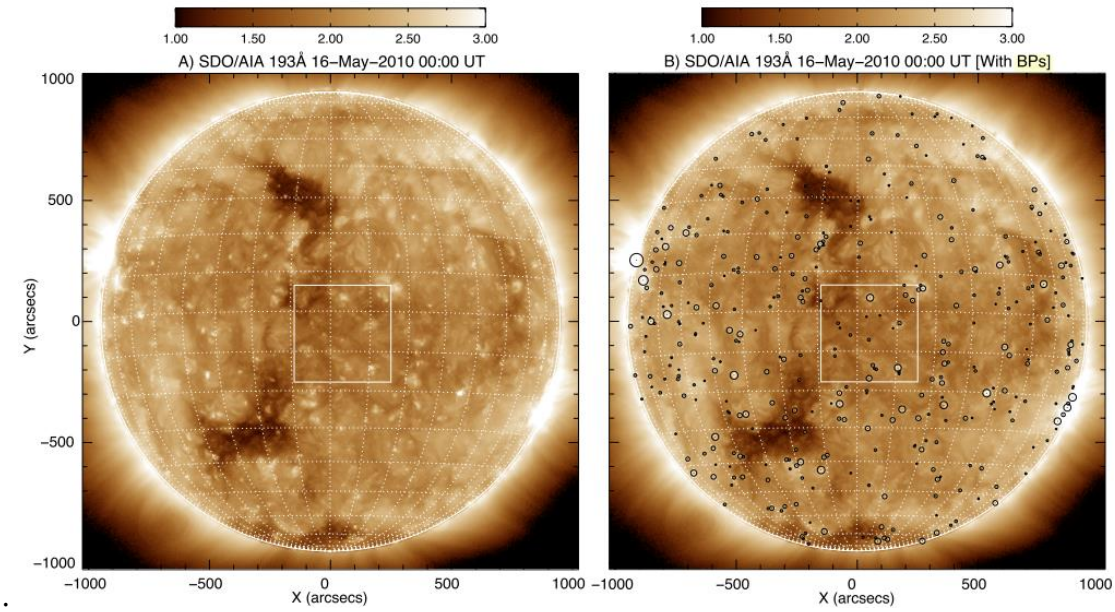

Figure 9: CBP's detection using BP-Finder algorithm. Image from (McIntosh, Wang, Leamon, & Scherrer, 2014), which highlights with circular shaped forms the CBP's

Regardless the previous approach, this algorithm as seen several modifications and improvements from different sources, (D. Sudar et al., 2015) (McIntosh et al., 2014), aiming to enhance precision and better execution times. Figure 9 represents one of those modifications and illustrates the identification of several CBP's across all altitudes, which is, apparently, a successful experiment. The methods used were focused on the pre-processing phase which prepares the image for some detection algorithm to be applied. These methods often hover the background intensity thresholds and most likely mixing images from different wavelength channels.

A more recent result when identifying CBP's is shown in Figure 10, which besides the relevant identification process of CBP's, (D. Sudar et al., 2015) also reveals some of the obstacles met using their modified BP-finder algorithm.

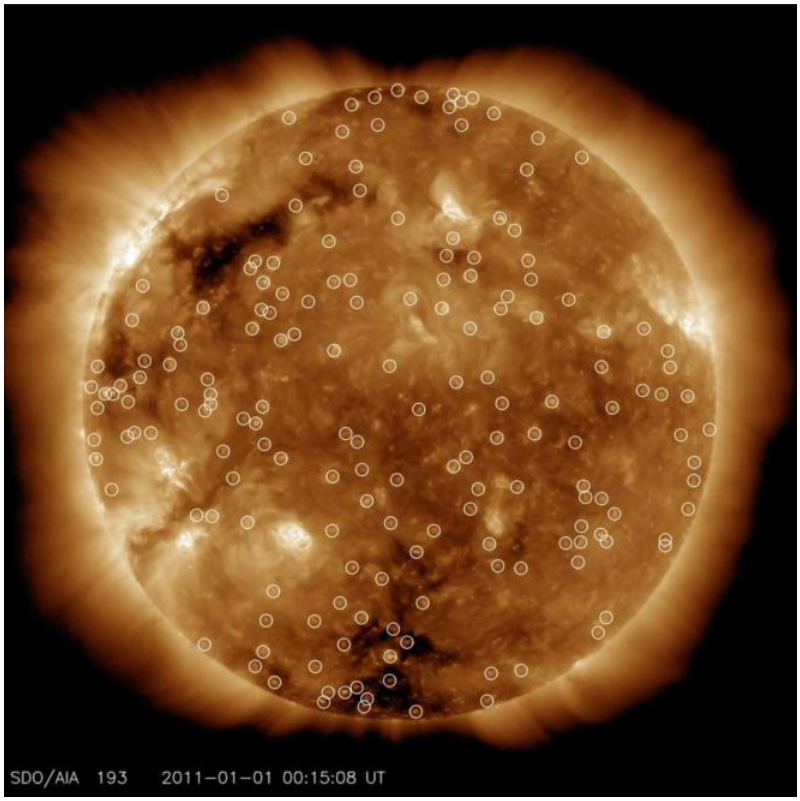

Figure 10: BP-Finder algorithm CBP detection Figure taken from (D. Sudar et al., 2015)

Despite most of the obstacles met were based on tracking, mostly due to instrumental capabilities, high or low cadence and data density, it is noteworthy to mention that larger errors occurred in active regions positions, where the algorithm demonstrated difficulties in detecting CBP's over a bright, variable background. Even so, (D. Sudar et al., 2015) conclusions, paraphrasing, "*The segmentation algorithm used here proved to be completely adequate for the task*" and delivered the necessary information to calculate Solar rotational profile with promising results.

2.1.3 PSO Snake Hybrid Algorithm

An efficient system capable of tracking and measuring solar features automatically was developed following a hybrid approach, which combines specialized image processing, evolutionary optimization and soft computing algorithms. The purpose, according to (Shahamatnia et al., 2016a), was to develop a system which provides detection, characterization and tracking.

Firstly and summarily, the evolutionary computation algorithm named Particle Swarm Optimization (PSO) is a search algorithm for finding the global minimum. PSO is a member of the family of stochastic optimization methods along with generic algorithms, between others. However, these type of methods does not guarantee finding an optimal solution, but rather the near

optimal solutions in very large spaces. Enthused by the social behavior in a flock of birds, the algorithm consists in relatively simple individuals, called particles, which each one of them represent a potential solution for the optimization problem. For better overall performance, PSO instead of searching in the whole space, looks for more promising areas, iteratively improving the candidate solutions until the final result. According to (Shahamatnia et al., 2016a), PSO algorithm outperforms others from the same family providing better efficiency, execution time and smaller number of functions needed to reach convergence.

Secondly and crucial point, a specialized image processing technique was included in the hybrid method. Naturally, image segmentation comes to mind when aiming to detect objects in digital images, consequently, it was added an active contour model known as "snake-model" and the contours are known as "snakes". The model works with energy functions, basically, every snake has its own energy and the one with lowest energy is considered the best match for representing the object.

2.1.3.1 Snake Model Process

The process starts with setting up the initial contour/curve, as previously mentioned, defining the snake, therefore, moving towards the object. The snake movement is overseen by internal and external forces, within the curve and from the image respectively. These forces are responsible for maintaining the snake shape and steer its way into the object. The Figure 11 represents the first step of the process, the snake being the initial contour and the object the target contour which is intended to detect.

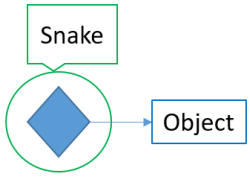

Figure 11: Snake model

The process can be illustrated by Figure 12, which is a step by step diagram:

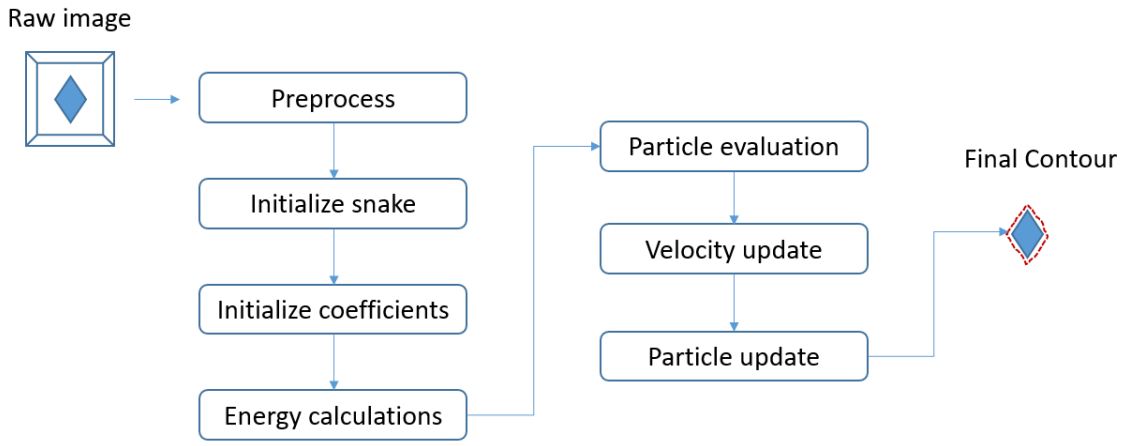

Figure 12: Snake model process

2.2 Tracking Methods

In this section, the author aims to provide an overall look on the literature about tracking features over a sequence of images. The purpose lies on identifying possible algorithms to be applied on the Sun's disk image in order to track CBP's. Considering a two-frame tracking example, tracking could be accomplished by using correlation-based matching methods, feature-based methods, optical flow techniques, change-based moving object detection methods between others. However, it is also needed to be considered the main difficulties about tracking in a reliable way, which can be caused by image noise, illumination changes, non-rigid motion, non-stable background and so on and so forth. Another important point to refer is that tracking involves two basic problems: Motion and Matching; Motion should predict the limited search region in which the feature to be tracked is likely to be in the next frame and Matching which is the detection methods previously discussed.

Given the fact that might be needed some sort of image evaluation process, image registration is a fundamental task often applied in image processing (Brown, 1992). The relevance of image registration lies on the necessity of comparing and integrate data obtained from different measurements, more precisely, if solar disk images from different wavelengths channels need to be correlated.

Lastly, the author would like to highlight Visual Based Algorithms to detect and track features, eventually to assist spacecraft's deciding autonomously the best landing sites. The applicability of these algorithms in detecting and tracking CBP's should be evident, both detection and

tracking algorithms coexist in the two purposes, despite the decision making behind choosing the best landing site being irrelevant for this dissertation.

2.2.1 Image Registration

Image Registration is the processed of overlaying images of the same scene but taken at different times. As previously mentioned, these type of processes are often valuable when correlating data from different measurements, therefore, introducing news aspects to analyze (Zitová & Flusser, 2003). According to (Zitová & Flusser, 2003) the majority of registration methods consists in the following four steps:

- Feature detection
- Feature matching
- Transform model estimation
- Image resampling and transformation

Bearing in mind the previous steps and neglecting the *Feature detection* due to already been discussed, clearly, some target template is needed to achieve *Feature matching*, which may or not be an obstacle due to storage or execution time constraints. Relatively to *Transform model estimation* it's the so called mapping functions which provide the means to define the types and parameters for aligning the two images. Lastly, *Image resampling and transformation* it is the transformation itself based on the previous parameters, whereas the resampling technique depends on the trade-off between accuracy and computational complexity. Often nearest neighbor or bilinear interpolation will be suitable for the task.

The detected features in the reference image and the sensed images can be matched using image intensity values in their close neighborhood. Usually, *Feature Matching* can be summarized into two major categories: Area-based and Feature-based methods. Area-based methods are often called correlation-like methods or template matching that often merge detection with the matching part. More often, this method inherit the disadvantages of template matching, for instance, there is a high probability of a window containing a smooth area to be matched incorrectly with other smooth areas in the reference image. In fact, looking at correlation methods which exploit matching directly image intensities, without any structural analysis, are sensitive to intensity changes which might be introduced by noise, varying illumination and other factors. Further techniques of area-based methods should be look in (Zitová & Flusser, 2003). Feature-based methods implying that the feature should already be detected and aim to find the pair wise correspondence using their spatial relation or various descriptors of features. Regarding spatial relations, are often applied when detected features are ambiguous or if their neighbors are locally

distorted. According to (Zitová & Flusser, 2003) there are some algorithms that use spatial relations, such as graph matching algorithm, clustering techniques and chamfer matching for image registration. On the other side, methods using invariant descriptors allow that correspondence of features may be detected based on specific features. These descriptors should be invariant, unique , should provide stability and be independent. Therefore, the simplest feature description is the image intensity itself, limited to the close neighborhood of the feature. Several descriptors are illustrated in (Zitová & Flusser, 2003) and mostly are based on deformations which are also frequently unique. Analyzing further into the same paper, some algorithms come across such as histogram of line-length ratios or histograms of angles differences.

Summarily, area-based methods are more likely to be applied to images that does not have many prominent details and the distinctive information is provided by gray level or color rather than shapes or structures. On the other hand, feature-based methods are typically applied when there is structural information available which are more significant than the image intensity. The common drawback are that feature may be harder to detect or are unstable in time. Therefore, it is crucial to identify its descriptors correctly.

2.2.2 Visual Based Algorithms

This sub-section aims to provide some context of autonomous image-based navigation algorithms to space science missions. The potential of these autonomous spacecraft systems is overwhelming, not only reducing costs but also enhancing other systems capabilities and perceptions. In fact, these systems are being developed to offer spacecraft's an autonomous approach to find suitable landing sites, also benefiting on-board systems with information about velocity and position relatively to a landing site (Johnson, Montgomery, & Matthies, n.d.). However, why is this important for detecting and tracking CBP's? The answer lies on the real-time detection and tracking of features during the descent of the spacecraft. Therefore, basically these systems and the one this dissertation aims to obtain settle in the same principles: detection of features, tracking them over a sequence of images and have a robust yet quick algorithm to fulfil its purpose.

According to (Johnson, 2014) there are two complementary technologies being developed to enable access to more extreme landing terrain during landing: Terrain Relative Navigation (TRN) for accurate positon estimation and Hazard Detection Avoidance (HAD) for avoiding small, unknown hazards. The image processing approach used by TRN include: image warping, feature selection and image correlation, which are components from the Lander Vision System (LVS).

In order to understand the following sequence of steps, Figure 13 will provide assistance based on the labels on it. Mainly, it will be discussed a Coarse Matching Method and Precision Matching Method.

Firstly, to contextualize the spacecraft is entering the planet (seen in label 1) and we have an overall view of the surface, generated a-priori using orbital data, which is a digital elevation map co-registered with an intensity brightness image (label2). From there, the image is normalized (label 3) to eliminate lower frequencies and enhance contrast for better matching. As the spacecraft is descending it takes several of images (label 4), but for the sake of the explanation lets only consider the first one. The next phase (label 5) is ignored due to not being relevant for this dissertation. Following the steps, the warped image is normalized (label 6) using the previous technique and it should be selected coarse features (label7) for matching against the normalized map (seen in label 3). As seen in Figure 13, under selected features square, there is a correlation template which will be submitted to a frequency based or Fast Fourier transformed-based correlation (label 8) in order to understand where that correlation matches the normalized map. The matching place will be a peak in correlation between the two datasets and therefore, use this information with the co-registered digital elevation map and create 3D points on the surface.

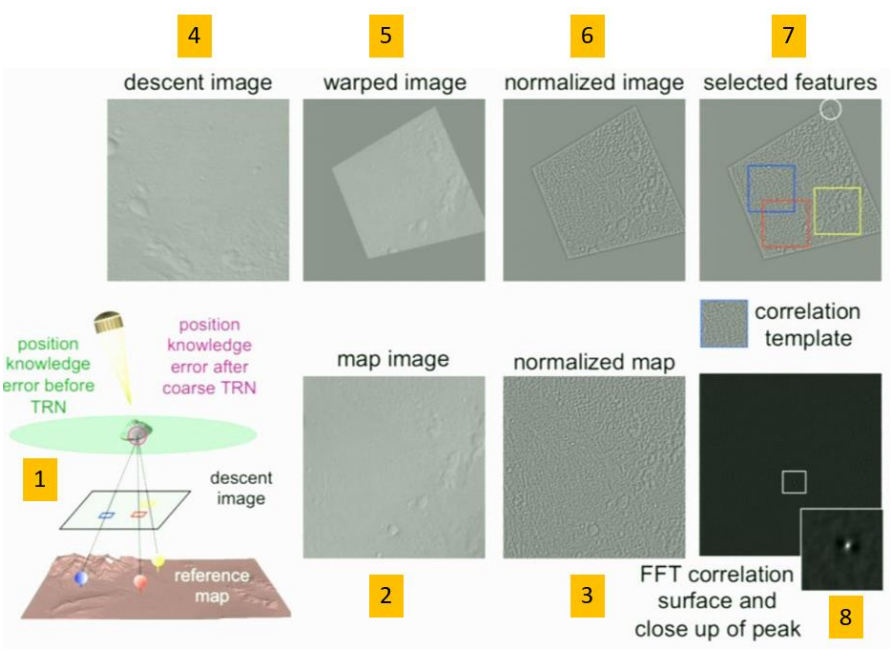

Figure 13: TRN image processing process. Courtesy of (Johnson, 2014)

More in detail, the normalization is used to reduce the differences in intensities between the descent image and the map image prior to correlation. There are some techniques such as low, high or band pass filters which will provide good results. Still regarding normalization, (Johnson,

2014) states that a simple and efficient approach is to compute mean and standard deviations of intensity or brightness in a local neighborhood around a pixel and subtract the mean and divide by the standard deviation an then applying it to the normalized map, shown in Figure 14.

$$\bar{p} = \sum \text{pi}\,, \qquad \sigma\text{p} = \sqrt{\sum (p - pi)^2}$$
$$p' = \frac{(p - \bar{p})}{\sigma p} \tag{2.2.1}$$

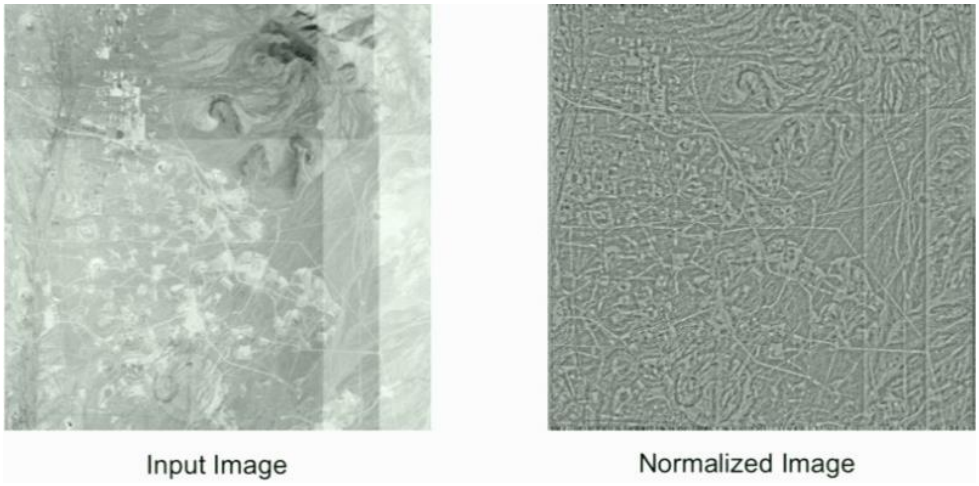

Figure 14: Normalization technique. Courtesy of (Johnson, 2014)

As seen in Figure 14, the purpose is to flat out everything and highlight the scene content, improving the overall processed while eliminating differences in brightness for example.

Regarding frequency domain image correlation the key issue is that frequency-based approaches are quicker in computation time over spatial correlation which is exactly what it is aimed to achieve – faster computation methods. The process is quite simple, basically transform the images into frequency domain, multiply them, do an inverse transform and find the peak. Figure 15 is an illustration of the process.

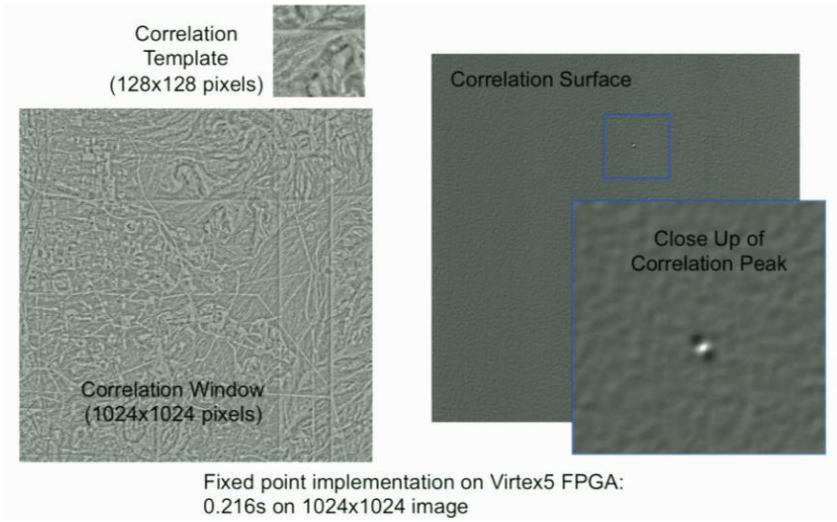

Figure 15: Frequency domain correlation Courtesy of (Johnson, 2014)

Concerning the Precision Matching Method, the process repeats itself and it is basically the same shown in Figure 13. However, in label 6, instead of a normalization, it uses an automatic processes that looks for possible locations for matching, which is called feature selection. This brings to a topic that is called Interest Operator, which according to (Johnson, 2014) is standard in computer vision and it is used to find locations in an image that are ideal for matching and tracking. Essentially it looks for strong gradients in image brightness in two direction in the image and the results can be seen in Figure 16. In fact, in the right side of Figure 16 what it aims to illustrate is the selected features in the blue circles, but also aims to explain that the system selects a feature in each grid cell and it clearly picks out bright areas, or like bright dots or even white blobs in a darker background. Eventually, some of these may have to be ignored but that's the main result of the Interest Operator.

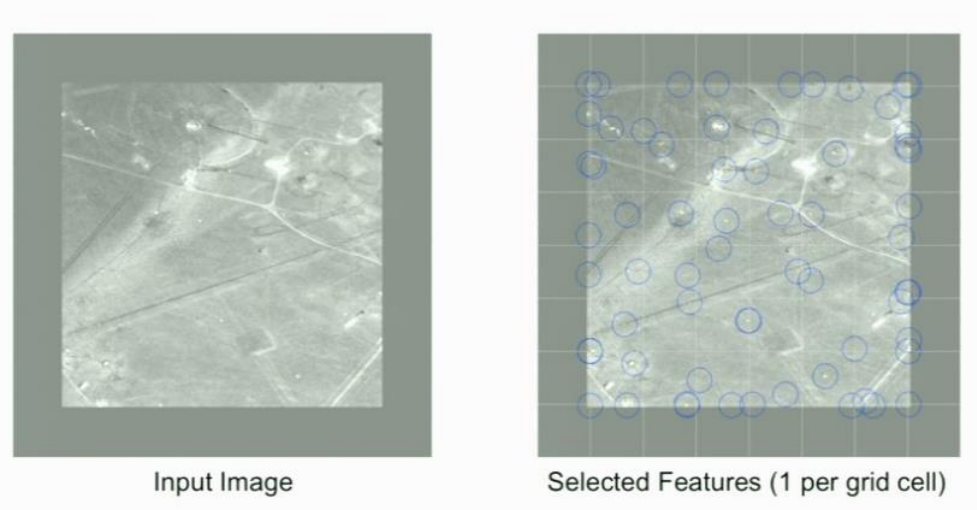

Figure 16: Interest Operator

Finally, by using both of Coarse Matching Method and Precision Matching Method and the correlation between the images and data from the two, the system is able to safely and accurately find the best possible landing spot in about 10 secs time, which an impressive time.

2.3 General Conclusions

The chapter covered some of the detection and tracking methods published, not only in the solar images case study but rather in a broader view related to advanced image techniques applied to different studies. It was also stated some of the obstacles faced by these methods in order to provide the reader and also the author with favorable insight about what should focused on while developing the software for this dissertation case study. More specifically, increasing CBPs detection accuracy towards other manifestations that might superimpose the tracers, or even taking into account the limb of the solar disk which deforms CBP appearance.

Based on the literature review about detection and tracking methods, Gradient Path Labeling algorithm should produce the best results for detecting CBPs. There is limited evidence that this algorithm will perform as accurately as it did in Druses or bacteria's due to never have been tested in solar images. Nevertheless, the promising results obtained by the algorithm might reflect bright results when applied to different case studies, such as solar features detection.

Regarding tracking, one of the most obvious and yet time consuming approach would be to apply some sort of template matching to every CBP and track it through a sequence of images. However, illumination, contrast, unprecise detection or differences in shape would increase both matching errors and processing time, resulting in an unfeasible process.

Another approach to tracking would be by securing an accurate detection, export all the CBP data to a process/database software and analyze the tracking through there. What is perfectly feasible because it should have all the parameters needed to characterize, select and track a given CBP.

It is noteworthy to mention that a correct image pre-processing is a major factor for the method's reliability. Applying a negative to the image, a specific filter, image contrast and illumination correction are common techniques applied by the author that deliver normalized versions of the original image to future processing.

3 Implementation

This chapter aims to describe implementation procedures, thought processes, challenges and solutions to overcome those challenges. Being the core of this dissertation, it scopes every aspect in detail, providing illustrations for quicker and more reliable understanding and introducing the reader to a further scientific and technical approach to the research problem.

3.1 Image Dataset

Image dataset is introduced as a subchapter under Implementation section due to its relevant significance acknowledged throughout the implementation phase. To begin with, a quick review on a few image formats is presented:

JPEG

Stands for "*Joint Photographic Experts*" group and it is a popular image file format often used by digital cameras. One of the many key qualities of JPEG is the possibility of multiple levels of compression which reduces the file size of the bitmap. This is accomplished with the loss of image quality, but it is the possibility to balance both quality loss and file size that makes this format so popular. Besides image data, JPEG files include metadata to describe file contents.

PNG

Stands "*Portable Network Graphics* and it is often used on the Web. This file format uses a lossless compression and provides 256 levels of transparency that distinguishes it from any other formats. Despite its many benefits it requires more disk space than JPEG, therefore, it is not suitable for every scenario being mostly used by web developers and graphic artists.

FITS

Stands for "*Flexible Image Transport System*" and it is the standard data format used in astronomy. It is used for transport, analysis, and archival storage of scientific data sets. FITS is known for its multi-dimensional arrays: 1D spectra, 2D images, 3D+ data cubes; tables containing rows and columns of information and header keywords for descriptive information about the data. Like other standards, FITS usage in astronomy predates JPEG and PNG and has some desirable qualities that are often crucial for scientific data:

- stores more bits per pixel and also floating values;
- Storage arbitrary number of data channels;
- Lossless compression;
- Storage unlimited metadata in the header.

It is therefore clear that FITS format co-evolved with astronomical data processing. FITS file compression is achieved using GZIP utilities.

Regarding the data it is imperative to talk about the star and the satellite responsible to supply that data. The Sun is often more interesting to be observed at Extreme Ultra-Violet (EUV) wavelengths, rather than visible wavelengths. This is particularly important when the object of study are Coronal Bright Points which appear bright in these wavelengths. NASA's Solar Dynamics Observatory (SDO) was launched aboard an Atlas V rocket on Feb. 11, 2010 with the mission to study the Sun's Energy and influence on space weather. Equipped with an Atmospheric Image Assembly (AIA) module it supports researchers through images in EUV wavelengths suitable to study Sun manifestations.

For this work, the data used was provided by SDO/AIA over three days, from 09/08/2010 to 11/08/2010 and from two different channels, to detect and track CBPs. This sequence of images show the sun full-disk as seen in the 19.3 nm channel of AIA, with 10 minutes interval between two consecutive images and a resolution of 4096 by 4096 pixel images. Although the original files were in the FITS format, these were converted to JPEG format with lossless compression, in

order to be opened in the developed application. FITS image header provided additional information such as: Sun radius ($R_\odot$), which is about ≈1578 pixels, the Sun is centered in the image and even the Sun distance from Earth which was 149,597,870,691.0 meters for the first image on the 9th of August, 2010.

Despite the use of full-disk images, data points near the limb (> 0.962 $R_\odot$) were not considered to avoid possible inaccuracies in position for this points.

3.2 Proposed Methodology

The following figure summarizes the proposed methodology which is divided into pre-processing methods, segmentation algorithm, post processing and a data evaluation approach to increase the CBP detection efficiency.

To build this methodology several attempts were made to understand what would be the most favorable path to decrease uncertainty, improve the segmentation procedure as well as the complete process. One of the challenges was to avoid active regions, known for being very bright and with several kilometers wide structures, where CBP detection is not clear due to the high amount of manifestations superimposed. Whether it should be avoided earlier or after the segmentation procedure is one of the strategies explained in this topic. Another challenge faced was related to the use of a decision tree as a final CBP selection, not only to understand what set of parameters needed to be considered, but also where across the whole process the decision tree should be implemented. Nevertheless, the final proposal is a suitable solution for most of the challenges encountered and provided the expected outcome.

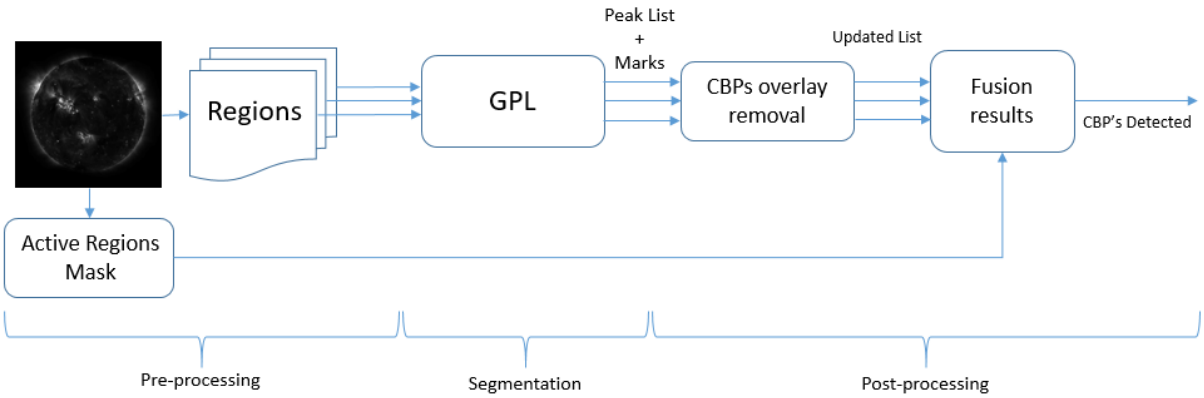

Figure 17: Proposed methodology

3.2.1 Pre-Processing

Due to the available high resolution images of the Solar disk (16 megapixels) and the segmentation algorithm complexity being proportional to the images resolution, the author chose to split the image into several smaller regions and apply the segmentation in each one of them. Fundamentally, this approach enables quicker processing when applied to a large dataset. However, there are a couple of particularities that need to be addressed, in order to, ensure no CBP is neglected.

First and foremost, the images available in the dataset used are 4096 × 4096 pixels and the Solar disk is centered, therefore, one of the first steps implemented was to discard unwanted regions like the borders of the image. In Figure 18, the original image was cropped in width and height around 440 pixels, which significantly reduces the number of pixels to be further processed. The selected region would therefore start in (x,y)=(440,440) pixel coordinates and finishing by the coordinate (x,y)=(3656,3656).

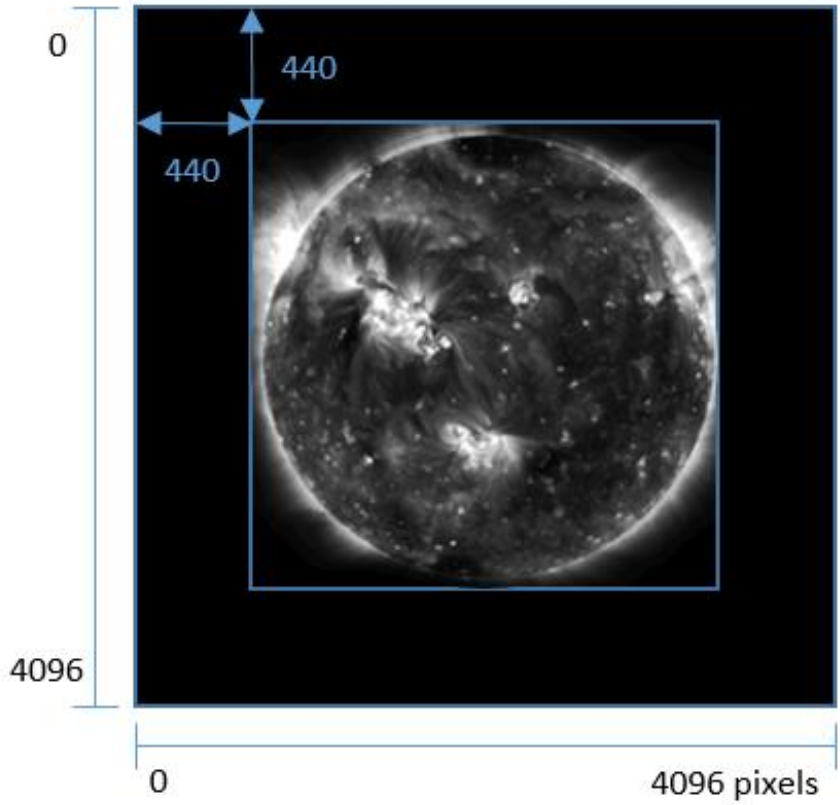

Figure 18: Discarded borders

Secondly, the remaining image still had to be cropped into regions as previously stated. For that reason, let us consider the following image, Figure 19.

Figure 19: Cropped image into two regions (Not in scale)

Figure 19 is an image from SDO 193 channel which was used for testing and to illustrate one of the challenges that led to a sliding window approach.

In spite of the sliding window approach, which will be discussed in the next subchapter, another challenge that can be perceived from Figure 19 is if a CBP is in the middle of the two regions. Ultimately, this issue can be addressed overlapping the two regions by a given percentage. Afterwards, when analyzing the data, the overlapping regions need to be carefully inspected for CBP's and verify if there are no duplicates. Both horizontally and vertically the overlapping was applied as seen in Figure 20 and Figure 21.

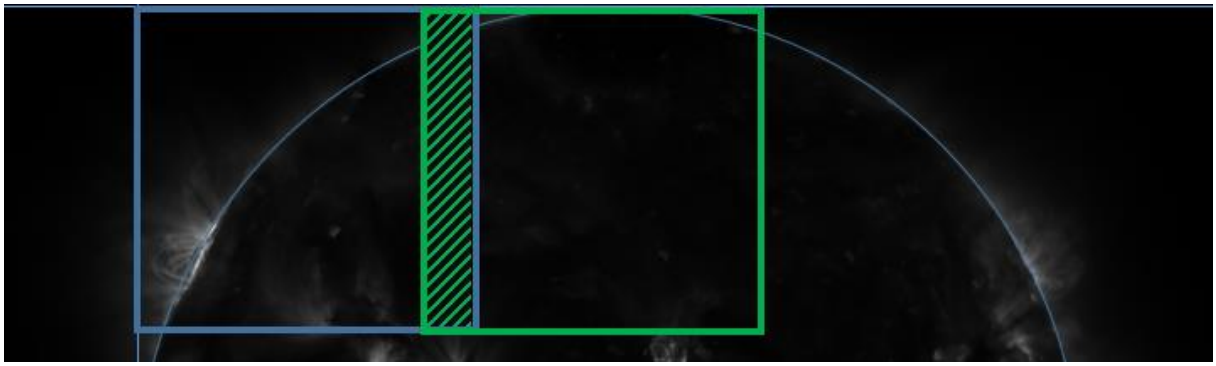

Figure 20: Cropped image horizontally with overlap(Not in scale).

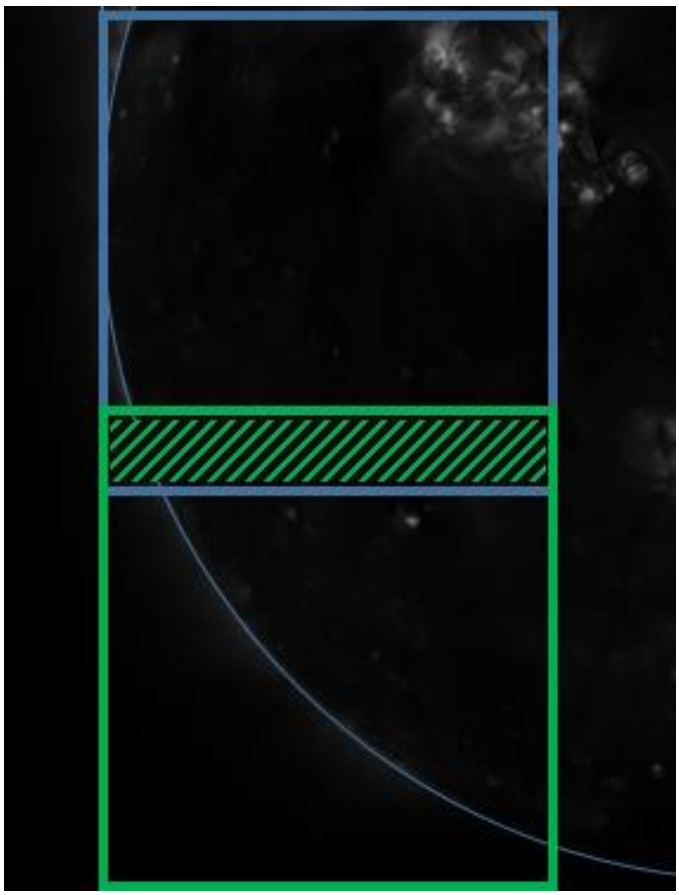

Figure 21: Cropped image vertically with overlap (Not in scale).

3.2.1.1 Sliding Window

As stated previously, a sliding window approach was followed to overcome the processing time constraints, hence, the images resolution.

After cropping borders the image sized reduced from 4096 × 4096 to 3216 × 3216, which is a 38.3% reduction. The reduced image had to be split into regions of the same size, taking also into account the overlapping area. For that reason, the reduction was actually about 15.73%.

The sliding window configuration began by understanding the pixel area of the CBP's (from 50 to 1000 pixels), to estimate how much overlapping area was required. Through visual inspection most CBP's would range from 30 pixels to 150 pixels, thus, regions would be overlapped in no less than 181 pixels, about 19%. The window size was also a factor, due to 181 pixels overlap and the requirements of being under 1024 × 1024 pixels, resulted in a window size of 940 × 940 pixels, as illustrated in Figure 22 which shows the calculations performed in both width and height. With this type of arrangement, the 3216 × 3216 pixels image is divided into 16 regions of 940 × 940 pixels.

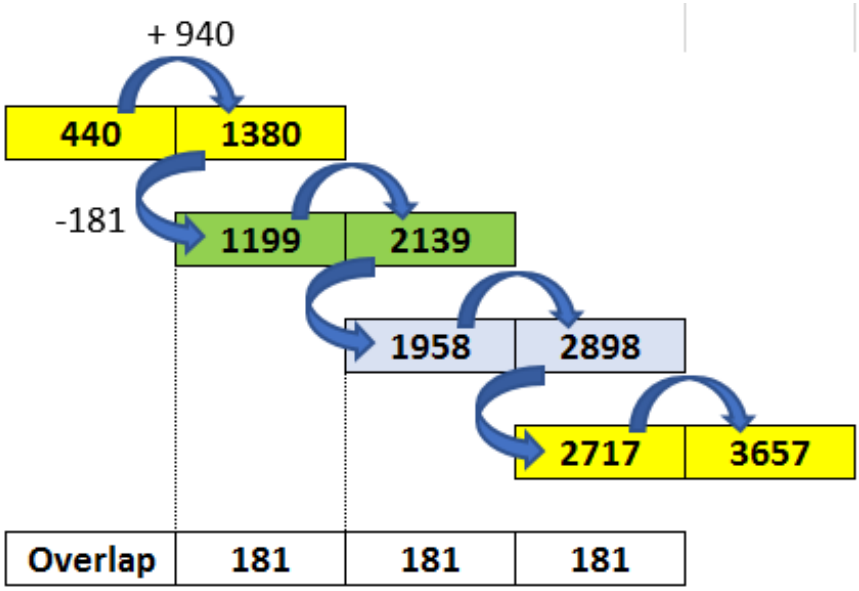

Figure 22: Overlap calculations

3.2.1.2 Active Regions Mask

Active regions, as previously explained in chapter one, are regions known for intense magnetic fields that emerge from the surface and can be easily spotted in sun disk images due to its brightness nature.

Initially, the first approach was to apply the segmentation algorithm and assess if the CBPs detection was accurate despite other bright manifestations. Truthfully, even after applying filters based on size, the algorithm outcome would exhibit CBPs inside active regions, which can be explained by existing inside these regions contours very similar to CBPs structures.

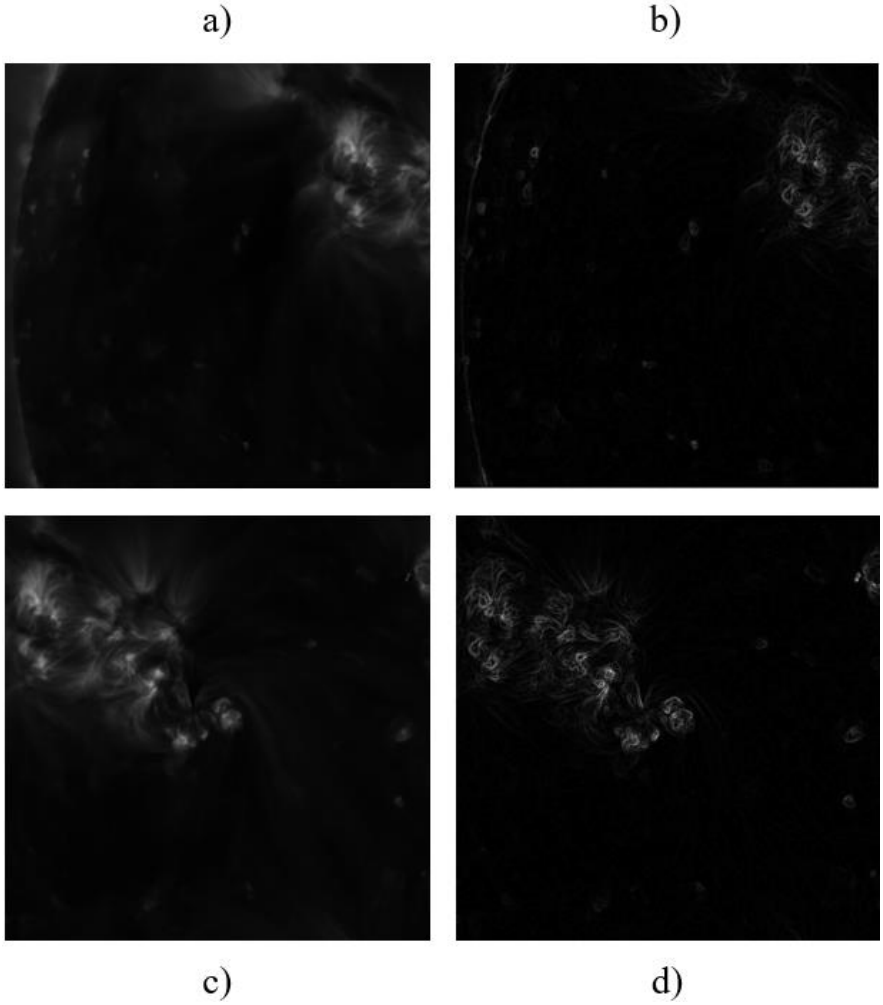

Figure 23: Solar images with and without Sobel filter applied. (a,c) Solar images before applying Sobel Filter. (b) CBP contours visible (on the left side near the limb) after Sobel filter application and an active region on the top right corner. (d) Active region represented after Sobel filter been applied.Both left images (a) and (c) are cropped images (not in the same resolution) from the original image that suffered a Sobel transformation resulting in the right side images (b) and (d). The issue focused on these illustrations lie on the visual structures seen in an active region, shown in d), which resemble the CBP structures shown in image b) (near the limb on the left side).

Some of the previous works done on CBPs detection stated that they discarded active regions as a result of being bright agglomerations of activities, which may or may not superimpose CBPs. Therefore, alongside with other authors, a binary mask was applied to remove active regions and the sun disk limb.

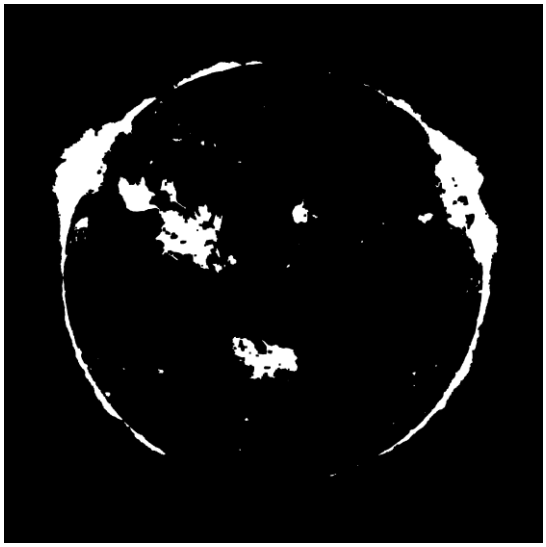

Figure 24: Sun disk binarization

Figure 24 illustrates the result image after binarization and morphological operations, namely erosion and dilation. More in detail, it was performed over a 2x2 mask an erosion and dilatation afterwards in the binary image. It could also have been used a greater mask, for instance 3x3. This mask would then be used to discard the CBPs selected inside the white regions, as follows: if the centroid of the CBP is located in a white pixel, then it should be invalid and, therefore, discarded.

Both morphological image processing operations used are useful to remove CBPs from the binarized image and thus accidentally rejected. These two transformations often used for image enhancement are used to decrease low amplitude noise and to remove smaller bright structures (CBPs) from the image.

The limb of the Sun image is a region where CBPs will appear stretched or with uncharacteristic structures, hence, potentially increasing detection inaccuracy. In order to minimize this issue and, again, following other authors, limb regions are neglected.

3.2.2 Segmentation

In 2.1.1 it is presented the segmentation algorithm used in this dissertation. Gradient Path Labeling algorithm was previously applied for detecting Druses in the human eye (A. D. Mora et al., 2011), to detect bacteria in a sample (A. D. Mora et al., 2015) and now to detect CBPs.

As explained previously, the original image is split into 16 sections where the GPL will be applied individually. This is the process of CBP identification and it was important to define which parameters should be addressed and are the most suitable for CBP detection. Some of those

parameters are location (offset X and Y), centroid location, pixel area, max, min, mean and accumulated amplitudes, gray and RGB mean and max amplitudes, validation criteria and label ID.

First and foremost, GPL configuration manager provides the user the option to do some image-preprocessing such as choosing from the source image one of RGB channels or its intensity. It also provides the option to apply negative, mean filter (3 × 3), gradient, use black as mask between other options. Secondly, after deciding which preprocessing need to be applied, the following options are related with the GPL configuration itself and the options available include 3×3 mean gradient or 5×5 gradient, flooding, merging amplitude percentage and merging min amplitude range. Thirdly, the options available are for results selection and are a set of filters that provide assistance for enhancing GPL results. This section includes min and max number of pixels that an object can have, min gradient amplitude, minimum ratio between gradient and pixel number, mean amplitude and even filter generated by decision trees.

The output of the GPL algorithm is, as previously mentioned, a collection of objects that represent the intended features for the detection. The GPL manager also provides visualization tools to better perceive the results, as well as saving options like exporting the data to an excel file.

Configuring the options available to obtain the most accurate CBP was key topic of this dissertation. Therefore, the configuration used was as follows:

Default values:

- Flooding = false;
- Flooding Stop Condition = 4;
- Lower Complete = false;
- Gradient 5×5 = false;
- Merge = true;
- Maximum Selection = false;
- Minimum Pixels = 0;
- Maximum Pixels = 0;
- Minimum Gradient Amplitude = 0;
- Minimum Amplitude = 0;
- Background = 85;
- Sectioning Threshold = 10;
- Amplitude Percentage = 5;
- Minimum Amplitude Range =3;

- Negative = false;
- Channel type =0;
- Mean filter = true;
- Outside Margin = 10;
- Use Black as Mask= false;
- Sort Max info = false;
- Watershed Marks = false;
- Watershed Immersion = false;

Changes for 19.3 nm channel:

- Negative = true;
- Gradient = true;
- Maximum Selection = true;
- Maximum Pixels = 50000;

Altogether it was assessed that the ideal configuration for GPL would somehow to select only small area objects with relatively high amplitude and ignore the remaining ones. Subsequently and regarding all the other amplitudes, they should be considered as in the same level, or the same plateau, which, therefore, created a big object that represents the background. The reason behind the change to 50000 pixels was to be able to detect the background instead of the CBPs, the outcome would be a massive object with gaps in it. Those gaps would, therefore, be possible CBPs. Essentially, after applying this change, each one of these gaps were validated on the existence of CBPs.

Regarding negative it is used to enhance white or gray details in dark regions. An Image gradient is a directional change in the intensity, which is aimed to detect the CBP contour, hence improving GPL results. In fact, the gradient analysis provide independence from illumination by searching for intensity changes and not just its amplitude, also allowing a significant reduction of noise artifacts.

It would be needed to adapt the GPL configurations for diverse channels due to the visual differences between them. Essentially, channel 131 is darker and with less easily identified CBPs by the human eye. Complementary to this statement an illustration of three sun disk images from three different channels is shown in Figure 25, which allows to understand the point made.

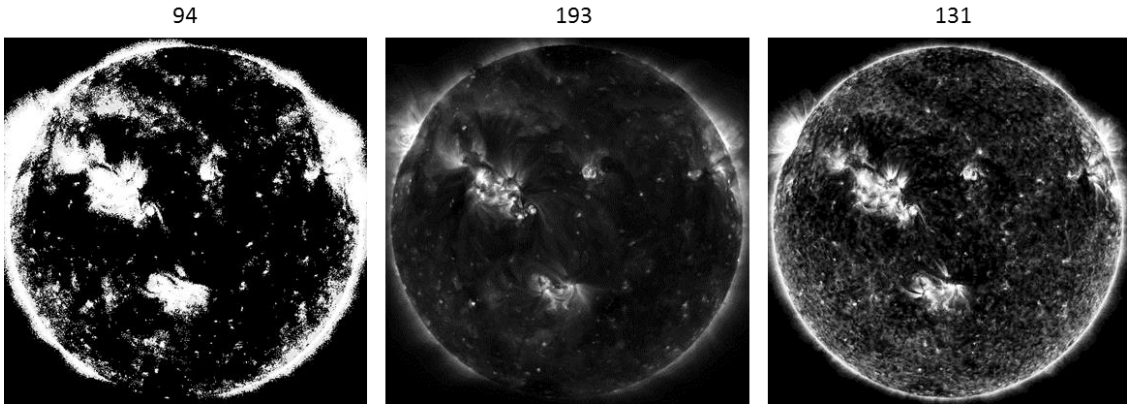

Figure 25: The Solar images obtained in 3 different SDO channels.

The primary focus of this post-processing is to gather the most important parameters that would allow to validate CBP detection and tracking through multiple sources, for instance, different wavelengths. If similar results were to be obtained would demonstrate the robustness of the algorithm and enhance the accuracy and precision of the detection. Another essential point is that for each wavelength some features are highlighted more than others, hence by extracting different information from all and fusion that data it is expected to improve the conditions to detect CBPs or even perceive events not acknowledged by individual inspection.

The segmentation can be synthetized into the insertion of GPL configurations, then proceeded by the actual detection process and finally a re-merge solution for improving results. To summarize Figure 26 illustrates the segmentation process.

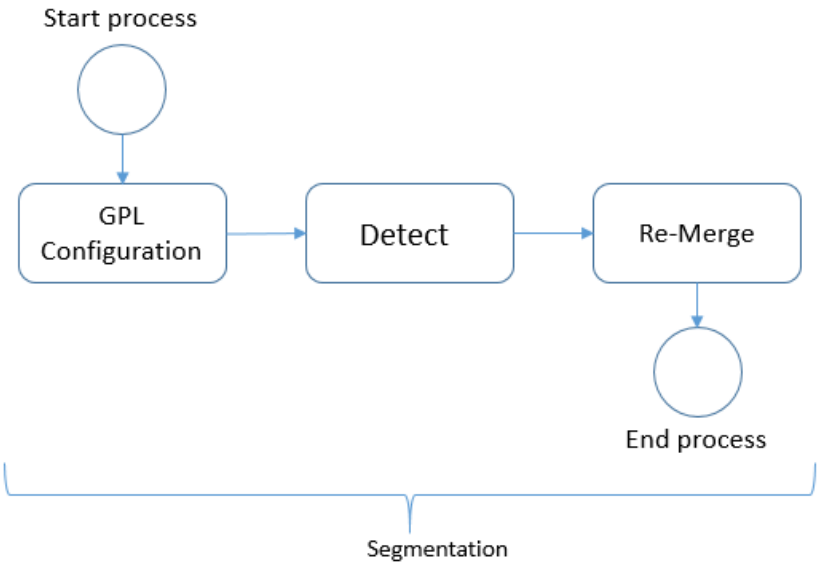

Figure 26: Segmentation process

Running the GPL detection with the first configuration set, it outputs an over segmented image that needs remerging to represent clear CBP structures, as illustrated in Figure 27. To achieve this, the amplitude percentage is changed to a greater value (e.g. 1000) in order to clear some unwanted objects.

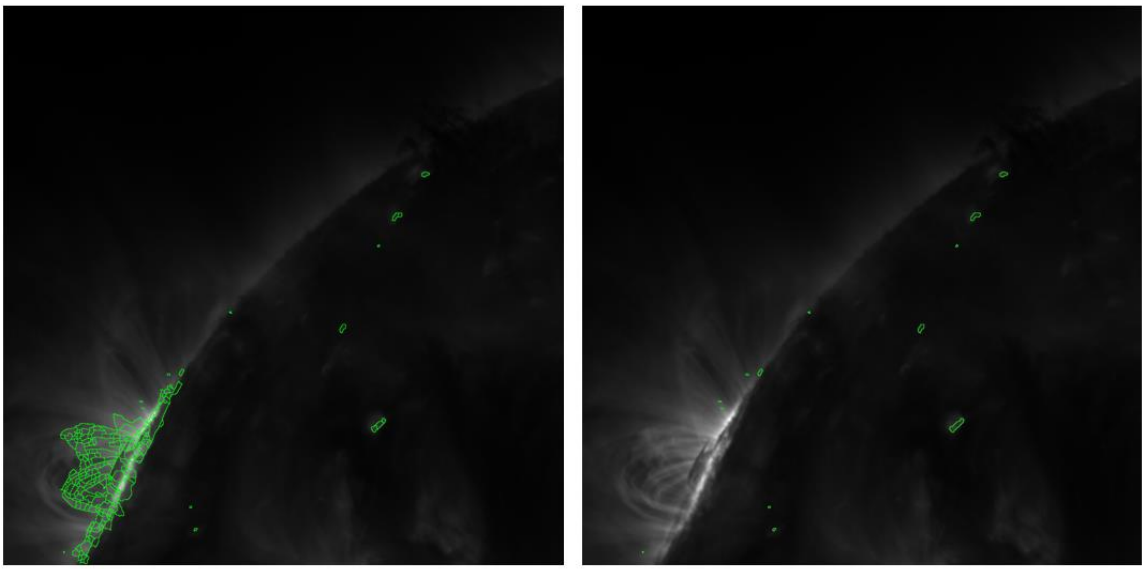

Figure 27: Remerge illustration. (a) Before merge, (b) after remerge;

In Figure 27 is also shown the removal of bright manifestations in the sun. On the left side of both images (on the limb), an active region is about to cross Earth line of sight with visible

prominences that were mistakenly selected by the algorithm. While in this case most of these unwanted objects would have been filtered by the binary mask, if any would have prevailed, this solution, yet not being perfect, would have helped in this matter. Additionally, as demonstrated by image b) (where no binary mask was applied) in the active region, that there are still some CBP size objects that prevailed, which would have been effectively discarded by the binary mask.

Figure 28 is another evidence of the remerged solution and illustrates in detail an object being remerged. Despite the validation for this object, the solution avoids the same entity being partitioned, which would increase inaccuracy.

Figure 28: Remerge close-up illustration. (a) Before merge, (b) after remerge;

Although these factors contribute to significantly improve the algorithm results, the cost is doubling its execution time. In conclusion, merge operation adds complexity and its execution time depends on the number of objects found initially, but it is a major factor for the algorithm successful output.

3.2.3 Post-Processing

Image Fusion is a methodology concerned with the integration of multiple images into a single image, usually more complex but suitable for human visual perception or specific computing processing tasks.

Post-processing in this document will cover the subject of retrieving data from a given channel, for example, 193 channel, and fuse it with the filters created, obtaining new peak list as illustrated in Figure 17. This is an important step to ensure the new peak list is as accurate as possible, containing every CBP and every parameter that makes it a CBP.

3.2.3.1 CBPs Overlay Removal

The sliding window approach was suitable to overcome the long processing time. However, splitting the image into 16 smaller regions overlapping each other by a given percentage, both in width and height, brought another problem of duplicate CBP detection.

Analyzing Figure 29 and recalling what was previously explained about the sliding window (e.g. overlay of 181 pixels), it is represented a section of 940 × 940 pixels with two painted sub-sections. One of 90 × 940 pixels (blue color) and another of 940 × 90 (yellow color). Finally, represented by the green color it is the intersection between the two sub-sections.

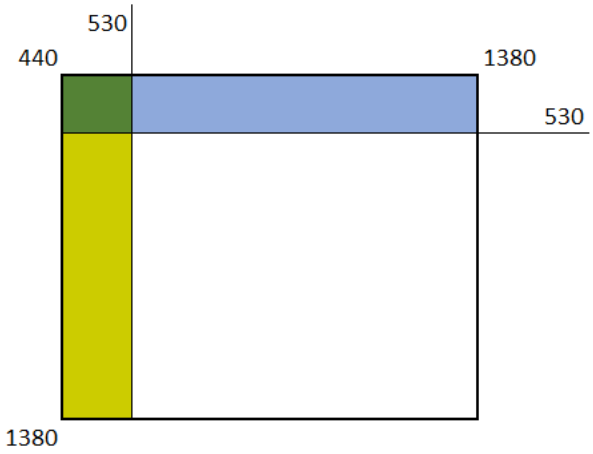

Figure 29: Section edges solution. Values in the image are in pixels.

In order to avoid duplicate CBP detections in the overlay area and still maintain assured that the sliding window concerns are met, CBPs centroids found before 530 (which is calculated by adding to the start pixel of the section half of the overlay value) will be discarded. This removes CBPs near the limb and also duplicated CBPs. This approach was applied to each 16 sections in the original image. The following figure (Figure 30), explains further the solution adopted.

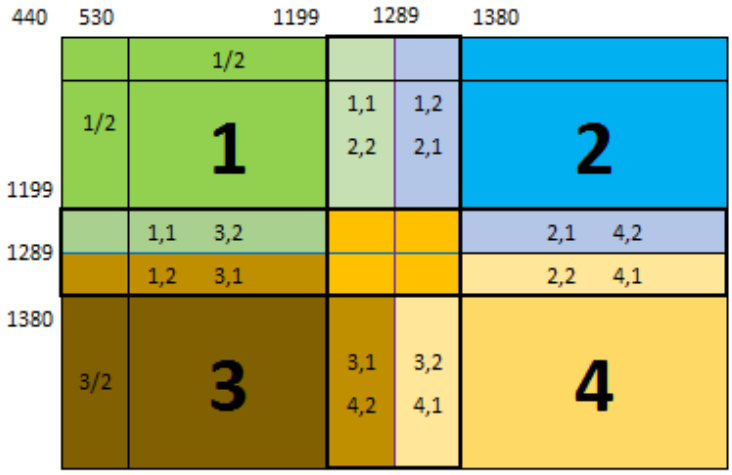

Figure 30: Overlay filter Values in the border of the image are in pixels, while inside the number represent different regions of the sections.

For example, Figure 30 shows 4 sections illustrated by the respective numbers. Regarding section number 1, it is noticeable six sub-sections represented by 1.1, 1.2 and ½. These sub-sections aim to demonstrate which part of the section will be evaluated for CBPs detection or removal. Accordingly, ½ sub-sections will be discarded as they are in the Sun's limb. Sub-sections 1.2 will be discarded and evaluated by section 2, as a result will prevent CBP duplication. Finally, sub-section 1.1 will be evaluated by section 1 and discarded by section 2, for example. Basically, this filter reduces redundant data as it avoids saving overlapping CPBs between edges of different sections.

In brief, the conditions are:

$$If(CBP\ is\ valid)\ and$$

$$if\ (Column < \frac{Overlay}{2}\ or\ Column \geq Width - \frac{Overlay}{2} \quad (3.1)$$

$$or\ Line < \frac{Overlay}{2}\ or\ Line \geq Width - \frac{Overlay}{2})$$

$$CBP\ is\ Invalid$$

4 Results Assessment

First and foremost, it is important to state that the nature of differential rotation of both solar surface and interior are still open issues of solar physics as (Dorotovic, 2012) states. Therefore, this chapter aims to explain and reveal the results obtained by detecting and tracking Coronal Bright Points and thus calculate solar rotational profile.

On a first phase, the accuracy of the detection algorithm was assessed by specialists. This was accomplished matching manual markings from two different specialists with the results from the automatic process. Consequently, this provided the necessary insight to understand CBP structures more precisely and ensure that the process was in the right path. The most important goal for this phase was to reach a matching criteria with the specialists about what is a CBP.

After tuning the process it was applied to 432 images (3 days) of the 19.3 nm channel, in order to retrieve the CBP information for each image. Each image divided into 16 smaller sections took up to 14 minutes to process and save the data into an excel file in a desktop computer with an i5 processor at 3.00 GHz, 8GB of DDR3 RAM and Windows 10 as operating system.

From these 432 images, 88034 CBP over 3 days were detected. For each CBP was saved: maximum intensity location, centroids, pixel area, maximum, minimum and differential amplitudes, RGB amplitudes, validation, filename and date. The time interval between two consecutive images was 10 minutes and the dataset started in 09/08/2010 until 11/08/2010. In Figure 31, it is shown the distribution of the detected CBPs for the 3 days and in a 4096×4096 pixel area.

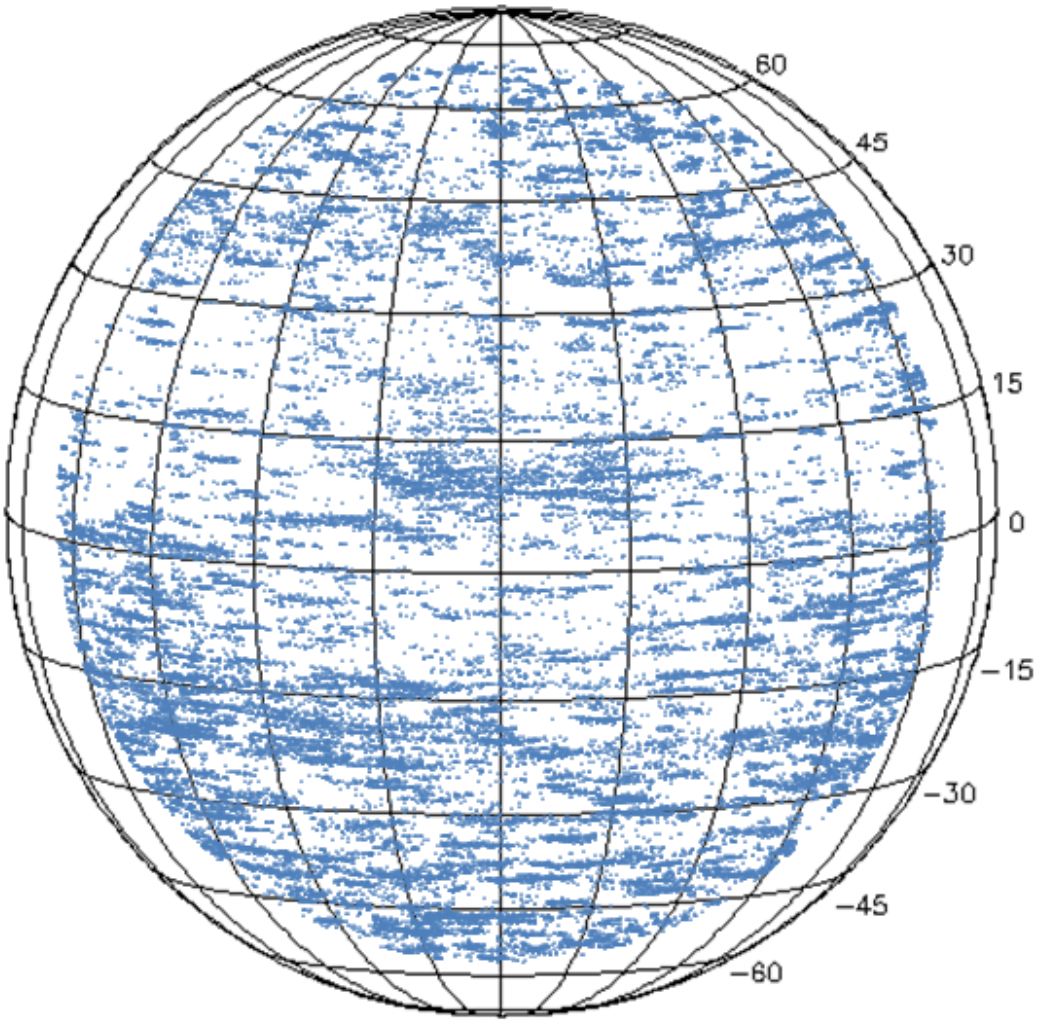

Figure 31: CBP data over 3 days (limb excluded) The tilt angle of the Sun related to Earth is ≈0,959. Stoneyhurst disks represent latitude and longitude in degrees

Analyzing the CBPs in Figure 31 a sense of motion can be perceived, perhaps more accentuated in some latitudes than others but still delivers a meaningful portrait of the CBPs that are aimed to be tracked. In contrast, Figure 32, represent a full disk image from august 09th of 2010.

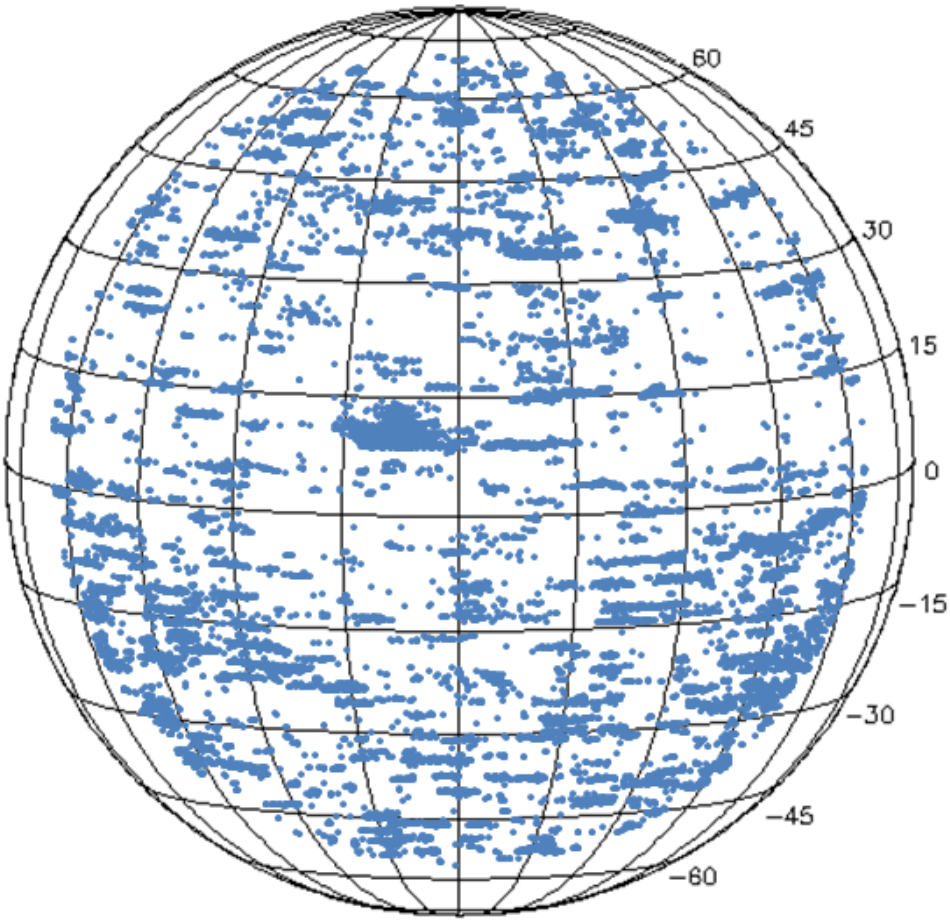

Figure 32: CBP locations on 9th August 2010 (limb excluded).

It is noteworthy to mention that the most valuable asset of CBPs that is being spread across every latitude is clearly shown in Figure 32. However, despite efforts on the removal of active regions, CBPs are still found near them, a clear sign of invalid CBP detection.

Furthermore, Earth does not orbit precisely over Sun's equator, so throughout the year the center of the Sun is tilted from Earth perspective. The grid shown in both Figure 31 and Figure 32 helps illustrating latitude and longitude. It is called Stoneyhurst disks, often used to overlay solar images and create reference lines to better perceive sunspots/CBP positions. Figure 33, illustrates the Stoneyhurst disk over the solar disk.

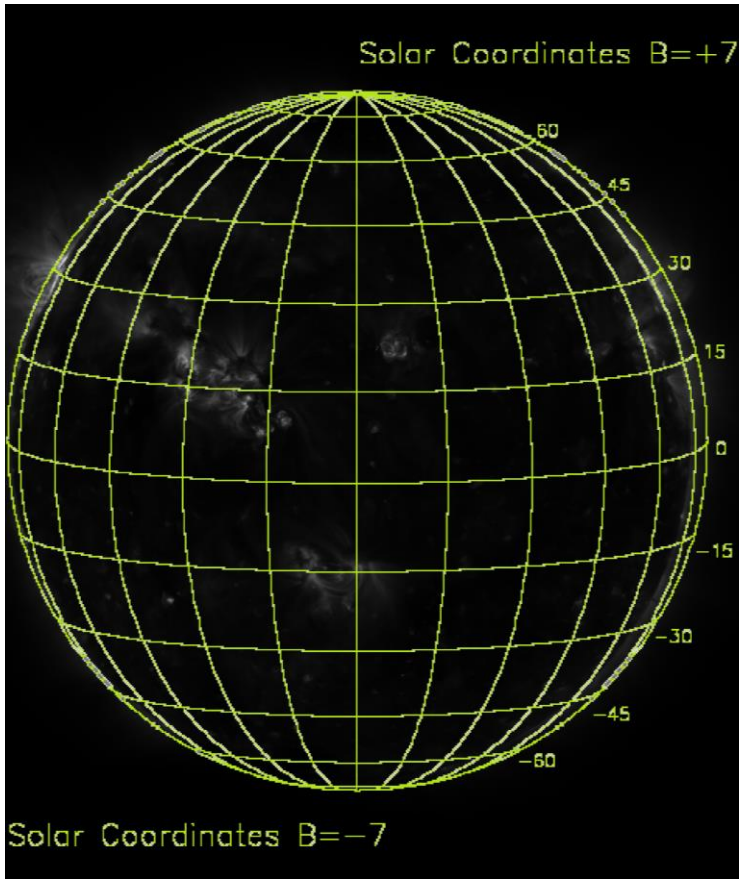

Figure 33: Stoneyhurst disks over solar image

The automatic process that uses GPL algorithm outputs coordinates in pixels that need to be converted in heliographic coordinates in order to study Solar rotational profile. Moreover, recalling what was previously stated in the last chapter, object positions near the limb would not be assessed due to being fairly inaccurate. Limiting data from 95% of the solar radius.

4.1.1 Methods and Equations

There are two basic methods to calculate Sun's surface rotational speed according to (Dorotovic, 2012): Spectroscopic method and tracer method. The first is based on Doppler equations and yields smooth results by the following relation:

$$\omega = A + \mathrm{B}\sin^2 b + C\sin^4 b \tag{4.1}$$

Where ω, is the sidereal angular velocity and A, B and C are constants in deg.day $^{-1}$.

The tracer method is based on observation of selected manifestations on the surface of the sun and tracking them in determined time intervals.

To be able to successfully retrieve Solar rotational profile based on tracers it is necessary to observe motion on a sufficiently long time interval, which means that not all CBPs found meet that criteria. There are several CBPs that are short lived and although they can be used, might not produce the best approximation of the Solar rotational speed.

The first step is to specify spherical coordinates b' and $\Delta l'$ of a given CBP in the image. For that, the solar radius, $R_{\odot}$, the CBP position, x and y, and the center of the solar disk, Cx and Cy are needed.

$$\sin b' = \frac{\mathrm{Cx}-\mathrm{Y}}{\mathrm{R}\odot} \qquad \sin \Delta l' = \frac{X-Cy}{\mathrm{R}\odot \times \cos b'} \tag{4.2}$$

For every measurement, Equations (4.2) and (4.3) are used to compute heliographic coordinate's b and Δl. The AIA images are already archived with the Sun centered and taking into consideration the positional angle of rotation axis, hence, the north of the Sun was always upwards. Another relevant point to highlight would be the tilt of the solar axis related to Earth which needed to be specific for the data used. For the days 09, 10 and 11 of August 2010, b value would be *b0*=6.3, *b1*=6.35, *b2*=6.41 respectively. Then these coordinates would be transformed into heliographic latitude b and angular distance from central meridian Δl.

In order to calculate the rotational profile and estimate the error the following equations were applied:

$$\sigma x = \sqrt{\frac{\sum(xi - \bar{x})^2}{n}}$$

$$\sigma y = \sqrt{\frac{\sum(yi - \bar{y})^2}{n}} \tag{4.3}$$

$$Rxy = \frac{1}{n \times \sigma x \times \sigma y} \sum \overline{(xi - \bar{x})(yi - \bar{y})}$$

Root-mean-square values σx and σy and the correlation coefficient Rxy were determined and used to retrieve the following least-square solutions by minimizing the residuals in the x and y directions, Kx and Ky.

$$Kx = \frac{Rxy \times \sigma y}{\sigma x} \qquad Ky = \frac{\sigma y}{Rxy \times \sigma x} \tag{4.4}$$

The synodic angular velocity, ω', of the structures was then obtained by Equation 4.5 in units of deg.day^{-1}:

$$\omega' = \frac{1}{2}(Kx + Ky) \tag{4.5}$$

Finally, to calculate sidereal angular velocity the equation is as it follows:

$$\omega = \omega' + \omega_E \tag{4.6}$$

Where ω_E is the Earth's orbital angular velocity.

4.1.2 Results Analysis

After running the CBP detection algorithm on the study image dataset (432 images), 8 CBP locations were selected manually across different latitudes and longitudes, taking into consideration the number of objects (at least 20) tracked to have their velocity measurements computed (Figure 34). This manual selection of a small number of CBPs provides evidence of the type of results that were to be obtained by the automatic procedure and, therefore, understand if the results are coherent with other authors on the same topic.

	Structure	n	b	wE	w
with Offset	a)	29	50,411	0,959	10,760
	b)	34	28,025	0,959	11,958
	c)	20	6,804	0,959	13,181
	d)	41	-16,396	0,959	13,632
	e)	26	-37,415	0,959	14,463
	f)	33	14,633	0,959	13,985
	g)	116	15,044	0,959	14,132
	h)	30	32,537	0,959	13,281

	Structure	n	b	wE	w
with Centroid	a)	29	50,367	0,959	11,320
	b)	34	28,053	0,959	12,668
	c)	20	6,831	0,959	13,080
	d)	41	-16,366	0,959	13,822
	e)	26	-37,389	0,959	15,069
	f)	33	14,657	0,959	14,094
	g)	116	15,045	0,959	14,339
	h)	30	32,569	0,959	46,059

Figure 34: 8 measurements from data collected. On the left, CBP is referenced by the maximum intensity coordinates (offset) and on the right using the centroid's coordinates.

Figure 34 shows 8 structures or CBPs (from a) to h)) with *n* being the number of images where this CBP was detected, *b* is the average heliographic latitude in degrees, ω_E refers to Earth orbital angular velocity, which is different for each day, and finally, ω denotes the computed angular rotation velocity in deg.day^{-1}. For ω_E it was used a fixed value of 0,959 degrees, no inter-

polation was required, since for these 3 days this value's change was below 0,0001. Also important to notice is the heliographic latitude disparity, in these 8 measurements the range in latitude goes from -37° to 50° which gives a good insight of the Sun rotation profile.

Another highlight in Figure 34 are the differences between offset and centroid measurements. Aiming to understand the differences between these two parameters in the angular rotation velocity calculus, these two tables were constructed and revealed that for some measurements the centroid might not be suitable, as it can be seen in CBP h) where the computed angular velocity, 46,059 deg.day^{-1} is clearly out of the acceptable range ([10-16]).

	n	w(offset)- w(Centroid)
a)	29	-0,56
b)	34	-0,71
c)	20	0,10
d)	41	-0,19
e)	26	-0,61
f)	33	-0,11
g)	116	-0,21
h)	30	-32,78

Figure 35: Relation between the values of angular rotation velocity.
Difference between values calculated from offset and centroid.

Figure 35 illustrates those differences and for most cases the value from the offset and the centroid is fairly equal. However, the measurement h) is a case where centroids lead to an incorrect angular rotation velocity. This type of error can occur if the object created by the GPL segmentation changes shape considerably, hence the change in centroid location or if the algorithm identifies the centroid outside the object and due to shape redefinitions the centroid coordinates change from a given position to other several pixels away. Nonetheless, in the majority of the CBPs both offset and centroid output approximately the same values, resulting in a difference lower than 1°.

Figure 36: CBP motion and Central Meridional Distance from offset measurements f) and h).

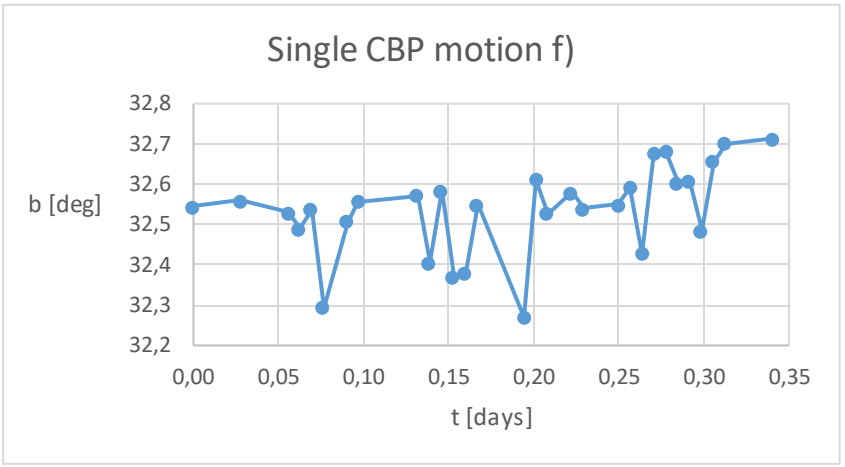

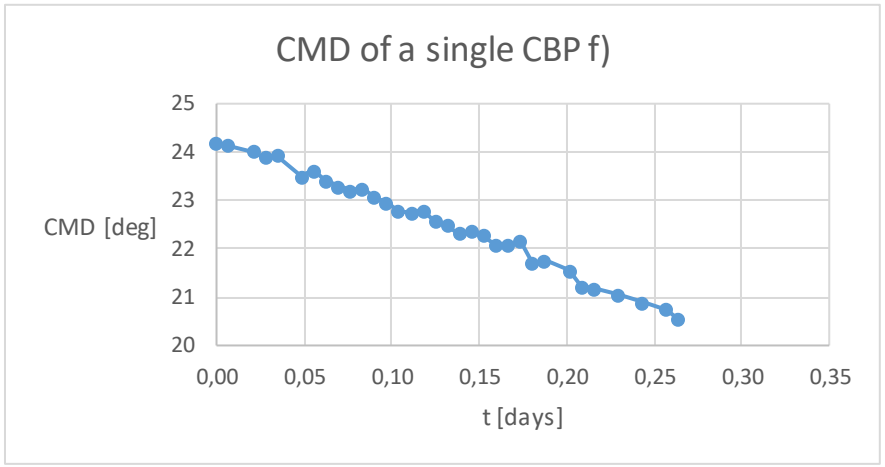

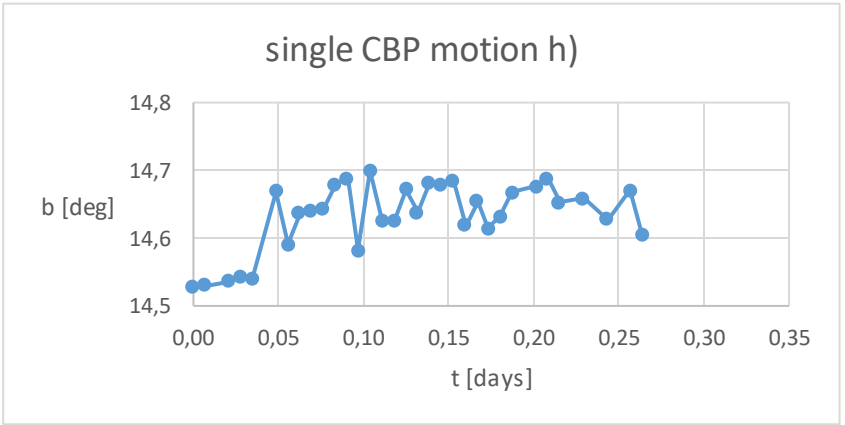

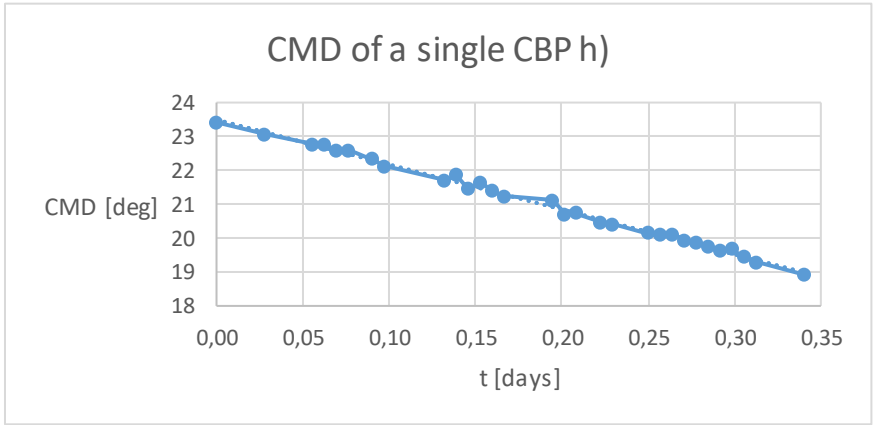

Figure 37: CBP motion and Central Meridional Distance from centroid measurements g).

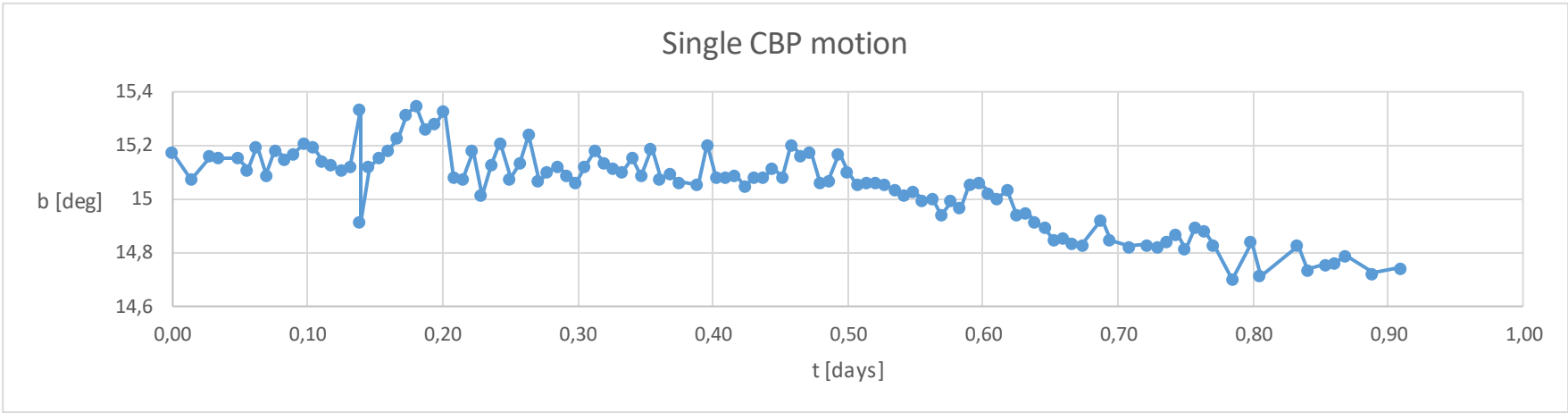

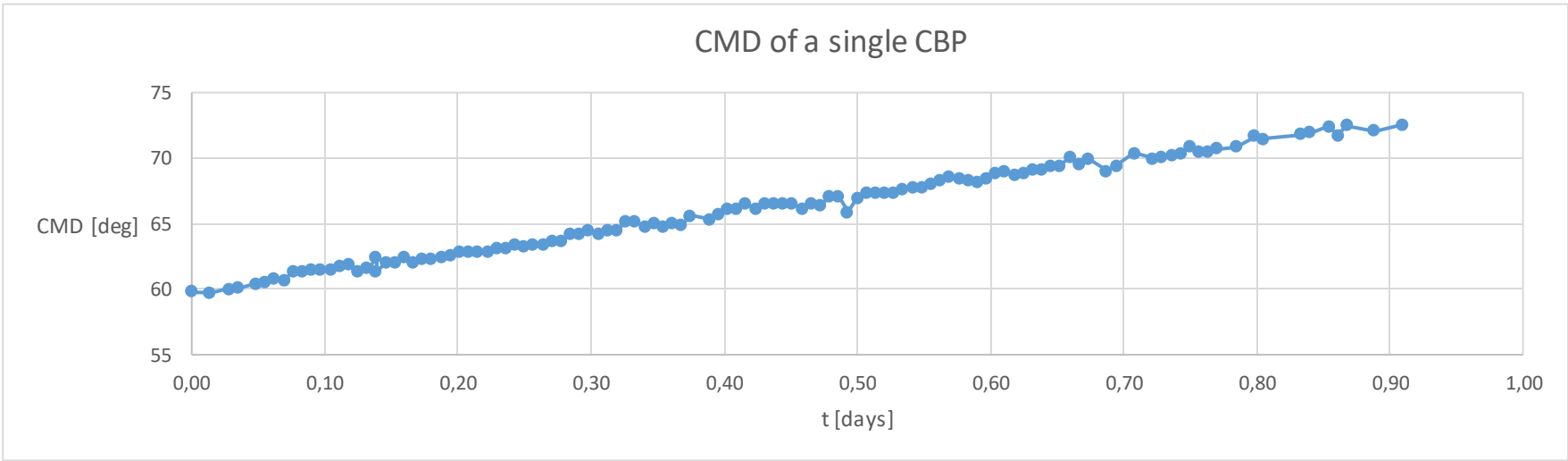

Figure 36 and Figure 37 show examples of processed data for different tracers. Figure 36 targets two tracers from different heliographic latitudes, namely ≈ 32° and ≈ 15°. Both tracers locate the object through the offset and track the CBP over 6 and 8 hours, respectively. These CBPs could be considered as short-lived due to the few hours visible in the solar disk. Still regarding Figure 36, in both tracers, central meridional distance is calculated and displayed.

Figure 37, on the other hand, displays the longer lived CBP from all the manual CBP selected. This tracer was tracked over 22 hours from 09/08/2010 to 10/08/2010 and the displayed chart was based on the centroid of the structure. This was important to show because centroid based CMD measurements produced, in some cases, the most linear distributions. Although, centroid based measurements exhibited promising results, in some cases, sudden changes in centroid positions produced wrongly velocity measurements.

The valuable insight that might be retrieved from both of these tables lie on the fact that either by tracing through offset, centroid or both, it produces satisfactory results when calculating angular rotational velocities. Nonetheless, due to a few unacceptable records when using centroid measurements and the lack of a decision method to choose between using offset and centroid in each case, it was established that offset measurements produced the best and more reliable results.

According to (Dorotovic, 2012) article presenting their results about the solar rotational profile, the following table was synthesized to match their records with the data obtained with the algorithm proposed in this dissertation. The data obtained by Dorotovic *et al.* and published in their article (Dorotovic, 2012) results from AIA 94nm channel and dates October 2010, 3 months apart from this dissertation dataset. Despite not having direct correspondence between the two data sources, which will introduce an error, it would still point out whether the results of proposed algorithm were similar to the ones previously published. The CBPs were selected from Dorotovic *et al.* article based on their latitude similarity with the corresponding CBP analyzed in this dissertation.

Table 1: Comparison of angular rotation velocities obtained from two sources.(Proposed algorithm and (Dorotovic 2012)).

Dissertation output			(Dorotovic 2012)			Δw
n	**b**	**w**	**n**	**b**	**w**	
29	50,4	10,76031	62	50,0	11,852	-1,092
30	32,6	13,28137	43	33,5	13,045	0,236
34	28,1	11,95798	86	27,8	14,478	-2,520
116	15,0	14,13157	80	15,6	13,941	0,191
33	14,7	13,98476	80	15,6	13,941	0,044
20	6,8	13,1809	190	6,4	14,340	-1,159
41	-16,4	13,63153	87	-20,0	14,205	-0,573
26	-37,4	14,46307	85	-36,4	13,812	0,651
					Mean value	-0,528

The differences, $\Delta\omega$, between the angular rotational velocity, ω, obtained with the proposed algorithm and one published by Dorotovic *et al.* are illustrated in the last column of Table 1. The average value -0,528 in deg.day^{-1} demonstrates that this dissertation output discloses an angular rotational velocity measurements approximately similar and therefore, precise enough to be used as a tracking method. However, further tests should be undertaken with more CBPs, hopefully with all the CBPs with a minimum of occurrences, to confirm these accuracy.

5 Conclusion and Future Works

This dissertation presented a methodology for detecting and tracking Coronal Bright Points in solar disk images using digital image processing techniques. The expected outcome was a fully autonomous tool with an accurate and reproducible system to reduce ambiguity amongst specialists.

Moreover, testing the Gradient Path Labeling segmentation algorithm in this case study was also an objective having obtained reliable results. The Gradient Path Labeling, initially developed to analyze retinal images (A. Mora, 2010), is a segmentation algorithm based on both Watershed Transform and Connected Components, using their advantages and sometimes exceeding their performances. Its ability to reliably adjust to different case studies is becoming one of its major accomplishments as demonstrated in this particular dissertation.

The Coronal Bright Points structures are sources of X-ray and ultraviolet emission recognized by small light dots. One of many specific traits about these structures is their special distribution across all latitudes which makes them one of the most important tracers to retrieve Solar rotation profile. One of the benefits of using the methodology proposed was the possibility to extract and store several parameters that describe CBP structures, which later can be a useful asset if a machine learning method is used.

In this dissertation, it was used 19.3 nm data from SDO/AIA instrument with a 10 min cadence, the GPL algorithm outputted approximately 88000 CBP locations over 3 days from 438

solar disk images. After applying filters to narrow the available data, it were selected 8 CBPs to compute solar rotation velocities. The results obtained had fairly good approximation when compared with values from other authors (Dorotovic, 2012)(D. Sudar et al., 2015). Despite the large density of data, the accuracy and robustness of the GPL algorithm enabled to track and measure velocities for short lived CBPs, which are more frequent than long lived ones. On the other hand, the developed tool capability of producing very high density data points in time, increased the algorithm execution time. For example, each 4096×4096 image took approximately 14 minutes to process in a desktop computer with an i5 processor at 3.00 GHz, 8GB of DDR3 RAM and Windows 10 as operating system.

Based on the results´ analysis it was inferred that the proposed tracer method for tracking CBPs produced reliable values of the rotational speed. Comparing the obtained tool results with literature results obtained for similar heliographic latitudes (Dorotovic, 2012) it were detected only small deviations of about 1 deg.day^{-1}. Although these comparative results are limited due to the small number of measurements presented, they display a promising reliability for the proposed methodology.

As often mentioned in this dissertation, the pre-processing steps have a fundamental influence on the algorithms performance as well as the quality of the dataset available. Notwithstanding its limitations it proved crucial to the results obtained, to normalize the dataset through filters applications to maximize its efficiency. Perhaps the downside of this work was the considerable amount of time spent on studying and analyzing the results from the data collected and therefore, being unable to provide a more insightful report.

It should also be mentioned the importance of the collaboration with astrophysicists from Slovak Central Observatory Hurbanovo, Slovakia, to understand CBP structures, their specifications and how visually challenging is to reliably detect them. The back and forth exchange of information allowed to perceive what type of tool was necessary to develop from a client point-of-view, in order to effectively support astrophysicists in their upcoming studies.

In summary, the developed tool enables gaining more knowledge about the solar structures and also to correlate the resulting data about Solar rotation profile with other studies. As explained previously, having access to better results about the surface motions of the corona is crucial for astrophysicists to understand the Sun internal and external manifestations.

5.1 Future Works

The development of a complete automatic tool for detecting and tracking CBPs still needs several improvements. The challenges lie not on the detection process (this was fully accomplished) but rather in the tracking and evaluation systems. Another challenge is that the images collected often require several pre-processing and since there are many possible wavelength images - suitable to study solar features - this a concern to be taken in consideration.

The most prominent improvement is related to tracking where the procedures used still have some issues to solve. Some of those issues could be solved by developing an algorithm/process that systematically and automatically detects sequences of CBPs over a determined period of time even in high density areas. Another issue is related to CBPs having a tendency of changing shape and size, which will increase the difficulty of its recognition and consequently, its tracking.

One important topic to mention is the slight disagreement between experts when manually selecting CBPs from a solar disk image, which understandably is not an easy task to accomplish. The work developed allowed to perceive that fusing data from different sources (different SDO wavelengths or other satellite images) would most likely enhance detection and remove some ambiguity.

More in depth on the method proposed, the algorithm used for detecting CBPs, Gradient Path Labeling could use an upgrade on handling higher resolution images, computation performance (which could be achieved by using multi-tasking) and other small add-ons. Many of the tracking and filter procedures used could, actually, have been merged into the tool, saving a lot of fastidious and unnecessary tasks. It is also noteworthy to mention that the binary mask applied to remove active regions, despite having accomplish its duty should be revised to improve results.

Finally, an automatic solution that included image fusion from different wavelengths to improve detection even in the most misleading cases, some type of learning method (e.g. decision tree) also to improve accuracy by gathering manual selections from multiple experts to create a solid learning pillar and lastly, data analysis and reports capabilities to assess and guarantee an accurate and reliable tracking system would be the ideal solution.

References

Acharya, T. (2005). *Image Processing Principle and Applications. ISBN: 13 978-0-471-71998-4*.

Brajša, R., Wöhl, H., Vršnak, B., Ruždjak, V., Clette, F., & Hochedez, J.-F. (2001). Solar differential rotation determined by tracing coronal bright points in SOHO-EIT images I. Interactive and automatic methods of data reduction. *A&A*, *374*, 309–315. http://doi.org/10.1051/0004-6361:20010694

Brown, L. G. (1992). A survey of image registration techniques. ACM Computing Surveys, 24(4), 325–376. http://doi.org/10.1145/146370.146374

Chandrashekhar, K., Prasad, · S Krishna, Banerjee, · D, Ravindra, · B, & Seaton, D. B. (2012). Dynamics of Coronal Bright Points as seen by Sun Watcher using Active Pixel System detector and Image Processing (SWAP), Atmospheric Imaging Assembly (AIA), and Helioseismic and Magnetic Imager (HMI), Solar Physics August 2013, Volume 286, Issue 1, pp 125–142. http://doi.org/10.1007/s11207-012-0046-1

D.Pandian, J. (2016). Does the Sun have a scientific name? (Intermediate) - Curious About Astronomy? Ask an Astronomer. Retrieved August 2, 2016, from http://curious.astro.cornell.edu/physics/49-our-solar-system/the-sun/general-questions/160-does-the-sun-have-a-scientific-name-intermediate

DeForest, C., & Lamb, D. (2014). SWAMIS Feature Tracking. Retrieved August 18, 2016, from http://www.boulder.swri.edu/swamis/

Deubner, F.-L. (1975). Observation of Low Wavenumber Nonradial Eigenmodes of the Sun. *SAO/NASA Astrophysics Data Systems (ADS)* , 371. Retrieved from http://articles.adsabs.harvard.edu/cgi-bin/nph-iarticle_query?bibcode=1975A%26A....44..371D&db_key=AST&page_ind=0&data_type=GIF&type=SCREEN_VIEW&classic=YES

Dorotovic, M Lorenc, M Rybanský I (2012). On Rotation of the Solar Corona, Solar Physics, vol. 281, issue 2, pp. 611-619. http://doi.org/10.1007/s11207-012-0105-7

Eddy, J. A. (1979). A New Sun: The Solar Results from Skylab. Retrieved August 3, 2016, from http://www.history.nasa.gov/SP-402/ch7.htm

Gurman, & McIntosh. (2004). EIT &EUV Brightpoints Over the SOHO Mission so Far. *Proceedings of the SOHO 15 Workshop - Coronal Heating. 6-9 September 2004, St.*

Andrews, Scotland, UK (ESA SP-575). Editors: R.W. Walsh, J. Ireland, D. Danesy, B. Fleck. Paris: European Space Agency, 2004., p.235, 235–240.

Johnson, A. (2014). Fundamentals of Image Processing for Terrain Relative Navigation (TRN). NASA NESC Academy Online. Retrieved from https://mediaex-server.larc.nasa.gov/Academy/Play/26381c8775954618b8ec8ae09574b90b1d

Johnson, A., Montgomery, J., & Matthies, L. (2005). Vision Guided Landing of an Autonomous Helicopter in Hazardous Terrain. Published in: Robotics and Automation, 2005. ICRA 2005. Proceedings of the 2005 IEEE International Conference https://doi.org/10.1109/ROBOT.2005.1570727.

Martens, P., Attrill, G., Davey, A., Engell, A., Farid, S., Grigis, P., … Thompson PCH Martens, B. J. (2012). Computer Vision for the Solar Dynamics Observatory (SDO). *Solar Phys*, *275*, 79–113. http://doi.org/10.1007/s11207-010-9697-y

McIntosh, S. W., Wang, X., Leamon, R. J., & Scherrer, P. H. (2014). Identifying Potential Markers of the Sun'S Giant Convective Scale. *The Astrophysical Journal*, *784*(2), L32. http://doi.org/10.1088/2041-8205/784/2/L32

Moon, K. R., Li, J. J., Delouille, V., De Visscher, R., Watson, F., & Hero, A. O. (2016). Image patch analysis of sunspots and active regions. *Journal of Space Weather and Space Climate*, *6*, A2. http://doi.org/10.1051/swsc/2015044

Mora, A. (2010). Advanced Image Processing Techniques for Detection and Quantification of Drusen.

Mora, Santinha, J, Gonçalves, N, Ribeiro, A & Fonseca, JM 2015, 'Detection and Segmentation of Nucleoids Based on Gradient Path Labelling', International Journal of Pharma Medicine and Biological Sciences, vol 4, no. 1, pp. 51-55.

Mora, A. D., Vieira, P. M., Manivannan, A., Fonseca, J. M., Hageman, G., Luthert, P., … Koch, G. (2011). Automated drusen detection in retinal images using analytical modelling algorithms. *BioMedical Engineering OnLine*, *10*(1), 59. http://doi.org/10.1186/1475-925X-10-59

NASA. (n.d.). NASA/Marshall Solar Physics. Retrieved August 21, 2016, from http://solarscience.msfc.nasa.gov/surface.shtml

Popova, H. (2015). Diminishing solar activity may bring new Ice Age by 2030 – Astronomy Now. Retrieved August 21, 2016, from https://astronomynow.com/2015/07/17/diminishing-solar-activity-may-bring-new-ice-age-by-2030/

Prigg, M. (2015). Nasa's Solar Dynamics Observatory | Daily Mail Online. Retrieved August 10, 2016, from http://www.dailymail.co.uk/sciencetech/article-2950009/The-incredible-video-reveals-five-YEARS-watching-sun-Nasa-s-Solar-Dynamics-Observatory.html

Redd, N. T. (2015). Space Weather: Sunspots. Retrieved August 3, 2016, from http://www.space.com/11506-space-weather-sunspots-solar-flares-coronal-mass-ejections.html

Shahamatnia, E., Dorotovič, I., Fonseca, J. M., & Ribeiro, R. A. (2016a). An evolutionary computation based algorithm for calculating solar differential rotation by automatic tracking of coronal bright points. http://doi.org/10.1051/swsc/2016010

Shahamatnia, E., Dorotovič, I., Fonseca, J. M., & Ribeiro, R. A. (2016b). An evolutionary computation based algorithm for calculating solar differential rotation by automatic tracking of coronal bright points. *Journal of Space Weather and Space Climate*, *6*, A16. http://doi.org/10.1051/swsc/2016010

Shahamatnia, E., Dorotovič, I., Mora, A., Fonseca, J., & Ribeiro, R. (2015). Data Inconsistency

in Sunspot Detection . In D. Filev, J. Jabłkowski, J. Kacprzyk, M. Krawczak, I. Popchev, L. Rutkowski, … S. Zadrozny (Eds.), *Proceedings of the 7th International Conference on Intelligent Systems IS'14* (Vol. 323, pp. 567–577). Cham: Springer International Publishing. http://doi.org/10.1007/978-3-319-11310-4

SOHO.Retrieved August 10, 2016, from http://sohowww.nascom.nasa.gov/classroom/classroom.html

Sudar, D., Saar, S. H., Skokić, I., Beljan, I. P., & Brajša, R. (2016). Meridional motions and Reynolds stress from SDO/AIA coronal bright points data. http://doi.org/10.1051/0004-6361/201527217

Sudar, D., Skokic, I., Brajša, R., & Saar, H. (2015). Steps toward a high precision solar rotation profile: Results from SDO/AIA coronal bright point data. *Astronomy & Astrophysics*, *575*(2012), A63. http://doi.org/10.1051/0004-6361/201424929

ThinkLink. The Sun ThingLink 24.3. Retrieved August 10, 2016, from https://www.thinglink.com/scene/718477462563979266

Thompson, M. J. (2004). Helioseismology and the Sun's interior. *Astronomy and Geophysics*, *45*(4), 4.21-4.25. http://doi.org/10.1046/j.1468-4004.2003.45421.x

Thompson, M. J., Christensen-Dalsgaard, J., Miesch, M. S., & Toomre, J. (2003). THE INTERNAL ROTATION OF THE SUN. *Annu. Rev. Astron. Astrophys*, *41*, 599–643. http://doi.org/10.1146/annurev.astro.41.011802.094848

Yogamangalam, R., & Karthikeyan, B. Segmentation Techniques Comparison in Image Processing. ISSN : 0975-4024.

Zell, H. (2015). Layers of the Sun. Retrived from https://www.nasa.gov/mission_pages/iris/multimedia/layerzoo.html

Zitová, B., & Flusser, J. (2003). Image registration methods: a survey. http://doi.org/10.1016/S0262-8856(03)00137-9